SKB

TECHNICAL REPORT 89-04

SKB WP-Cave Project
Radionuclide release from the near-field in a WP-Cave repository

Maria Lindgren, Kristina Skagius

Kemakta Consultants Co, Stockholm

April 1989

SVENSK KÄRNBRÄNSLEHANTERING AB
SWEDISH NUCLEAR FUEL AND WASTE MANAGEMENT CO

BOX 5864 S-102 48 STOCKHOLM
TEL 08-665 28 00 TELEX 13108-SKB

SKB WP-CAVE PROJECT
RADIONUCLIDE RELEASE FROM THE NEAR-FIELD IN A WP-CAVE REPOSITORY

Maria Lindgren, Kristina Skagius

Kemakta Consultants Co, Stockholm, Sweden

April 1989

SKB WP–CAVE PROJECT

RADIONUCLIDE RELEASE FROM THE NEAR–FIELD IN A WP-CAVE REPOSITORY

Maria Lindgren
Kristina Skagius

Kemakta Consultants Co
Stockholm, Sweden

April 1989

ABSTRACT

The release of radionuclides from the bentonite-sand barrier (near-field) in a WP-Cave repository for high level radioactive waste has been studied. Calculations were made for two cases; a Low Flow Through Case and a High Flow Through Case. The difference between the two cases lies in the assumed hydraulic properties of the bentonite-sand barrier and the system inside the barrier. The effect on the nuclide release of solubility limitations, sorption capacity of the barriers, radiolytic fuel oxidation rate as well as the thickness of the bentonite-sand barrier, were also investigated for the Low Flow Through Case.

TABLE OF CONTENTS

SUMMARY

The release of radionuclides from the bentonite-sand barrier (near-field) in a WP-Cave repository for high level radioactive waste has been studied. Calculations were made for two cases; a Low Flow Through Case and a High Flow Through Case. The difference between the two cases lies in the assumed hydraulic properties of the bentonite-sand barrier and the system inside the barrier.

The fuel dissolution and subsequent nuclide transport out from the repository will start when the steel canisters containing the fuel collapse. This was assumed to occur 200 years after repository closure. The liberation of the nuclides from the fuel was assumed to be determined by the radiolytic fuel oxidation rate. A conservative estimate of the fuel oxidation rate was used leading to complete oxidation of all the fuel in the repository (1100 tonnes) after $1.2 \cdot 10^6$ years. In calculations where solubility limits were taken into account, the source term for the nuclide transport was set to the solubility for those nuclides that would reach the solubility with the applied fuel oxidation rate.

The nuclide migration from the collapsed canisters to the water flowing in the rock outside the bentonite-sand barrier was modelled as transport by diffusion through finely ground rock surrounding the canisters in the canister channels and as transport by diffusion and advection through the bentonite-sand barrier.

With the hydraulic conductivities assumed for the Low Flow Through Case, the bentonite-sand will act as a diffusion barrier at times longer than about 5000 years after canister failure. At shorter times, release by thermally induced flow will predominate. The release during the first 10^6 years after canister collapse will be dominated by some of the non-sorbing and slightly sorbing fission and activation products. The level of the maximum release rate during this period lies between 10^{-2} and 10^{-1} GBq $\cdot$ a^{-1}, and is totally determinated by the release rate of carbon-14. The release at longer times will be dominated by the long lived actinides and daughter nuclides. With the solubilities used, the level of the maximum release rate will not exceed 10^{-3} GBq $\cdot$ a^{-1}. The predominant nuclides during this period are neptunium-237, plutonium-242 and uranium-233.

In the High Flow Through Case, higher hydraulic conductivities in the bentonite-sand barrier and in the interior part of the repository were applied. In this case the nuclide release from the bentonite-sand barrier will be determined by the water flow through the barrier. The water flow is composed of a thermally induced part and a natural gradient driven part. The water flow is decreasing with time due to a decrease in the thermally induced flow. The level of the maximum release rate during the first 10^6 years is calculated to be about 2-3 GBq $\cdot$ a^{-1}. The dominating nuclides during this period are the non-sorbing and slightly sorbing fission and activation products. At longer times the maximum release rate will be about 10^{-3} GBq $\cdot$ a^{-1} caused by the release of long lived actinides and daughter nuclides.

The increase in maximum release rate of dominating nuclides if the thickness of the bentonite-sand barrier is reduced from 5 to 2.5m has been estimated to be less than a factor of 5 in the Low Flow Through Case and about a factor of 2 in the High Flow Through Case. A higher fuel oxidation rate will only influence the maximum release rate of the non-solubility limited nuclides. A 5 times higher fuel oxidation rate in the Low Flow Through Case will increase the maximum release rate from the bentonite-sand barrier by a factor less than 2.

1. INTRODUCTION

The WP-Cave concept for storing high level radioactive waste has since April 1986 been under investigation as a part of the SKB research programme. The first phase of the study was devoted to define a repository design and to describe the function of the repository during construction, short term and long term storage. In the second phase, processes and events identified during the first phase to be of importance for the long term safety of the repository were studied in more detail. The outcome of Phases 1 and 2 has formed the basis for Phase 3 which comprises a safety analysis of the WP-Cave design.

The safety analysis can be divided into three parts:

- calculations of the nuclide migration from the fuel in the canisters to the water flowing in the rock outside the bentonite-sand barrier (near field transport) after canister collapse,

- calculations of the nuclide migration through the rock outside the bentonite-sand barrier to a drilled well or a lake (far field transport), and

- calculations of the biosphere transport from a well or a lake to the intake by man, and resulting dose exposure.

The objective of the work described in this report has been to study the nuclide migration in the near field, and to estimate the release rates from the bentonite-sand barrier of all nuclides expected to give a significant contribution to the radiation dose. The calculations have been focussed on a case referred to as the Low Flow Through Case, but the release rates of some dose important nuclides have also been determined for an alternative case referred to as the High Flow Through Case.

2. DESCRIPTION OF A WP-CAVE REPOSITORY

2.1 DESIGN

Two different sizes of a WP-Cave repository were originally proposed, WP-Cave 1500 and WP-Cave 3750, where the figures indicate the approximate capacity in tonnes of uranium. The calculations have been performed for a repository with the same dimensions as the WP-Cave 1500, but with the capacity reduced to 1100 tonnes of uranium. Following the naming convention this repository design should be called WP-Cave 1100. The continuing description is only valid for this size.

The shape of a WP-Cave can be compared with a huge egg, where the shell consists of a 5 metre thick bentonite-sand barrier, see Figure 2-1. The top of this barrier is located 200-250 metre below the ground and the distance between the top and the bottom of the bentonite-sand barrier is 300 metre. The outer diameter of the cylindrical part of the bentonite-sand barrier is 130 metre. The proposed mixture of bentonite and sand is 10% bentonite and 90% sand in the bottom part, 20% bentonite and 80% sand in the cylindrical part and 50% bentonite and 50% sand in the top part of the barrier. Because of possible problems with release of hydrogen gas through a 50/50 bentonite-sand barrier, also a mixture with only 10% bentonite in the top part of the barrier is considered.

Outside the bentonite-sand barrier a hydraulic cage is located. The cage is composed of tunnels and vertical bore holes connecting the tunnels with each other, see Figure 2-1. The hydraulic cage has a diameter of 230 metre and a height of 450 metre, and the distance to the bentonite-sand barrier is 50 metre.

The repository part is located in the centre of the volume inside the bentonite-sand barrier. It consists of a vertical central shaft with 12 vertical shafts placed along the circumference of a circle with a diameter of 26 metre (inner ventilation shafts) and another 12 shafts placed on the circumference of a circle with a diameter of 61 metre (outer ventilation shafts). The central shaft and the inner and outer ventilation shafts are connected through radial canister channels at 16 levels with 12 channels per level. The channels are sloping from the centre to the periphery, see Figure 2-2. In each channel two steel canisters containing the burned out fuel are placed. The height of the inner and outer ventilation shafts is 110 metre. All channels and shafts are purposed to be lined with steel plate.

The volume between the repository part and the bentonite-sand barrier consists of rock. The radial distance from the outer ventilation shafts to the bentonite-sand barrier is approximately 30 metre.

2.2 OPERATION

During the construction phase the whole system inside the hydraulic cage will be drained. This drainage will be continued during 100 years after loading the steel canisters. During this dry supervised period the canisters will be cooled with air.

After 100 years the drainage is terminated and the channels and shafts are refilled with finely ground rock and water. All connections to the surface are closed, and the long time storage of the fuel starts.

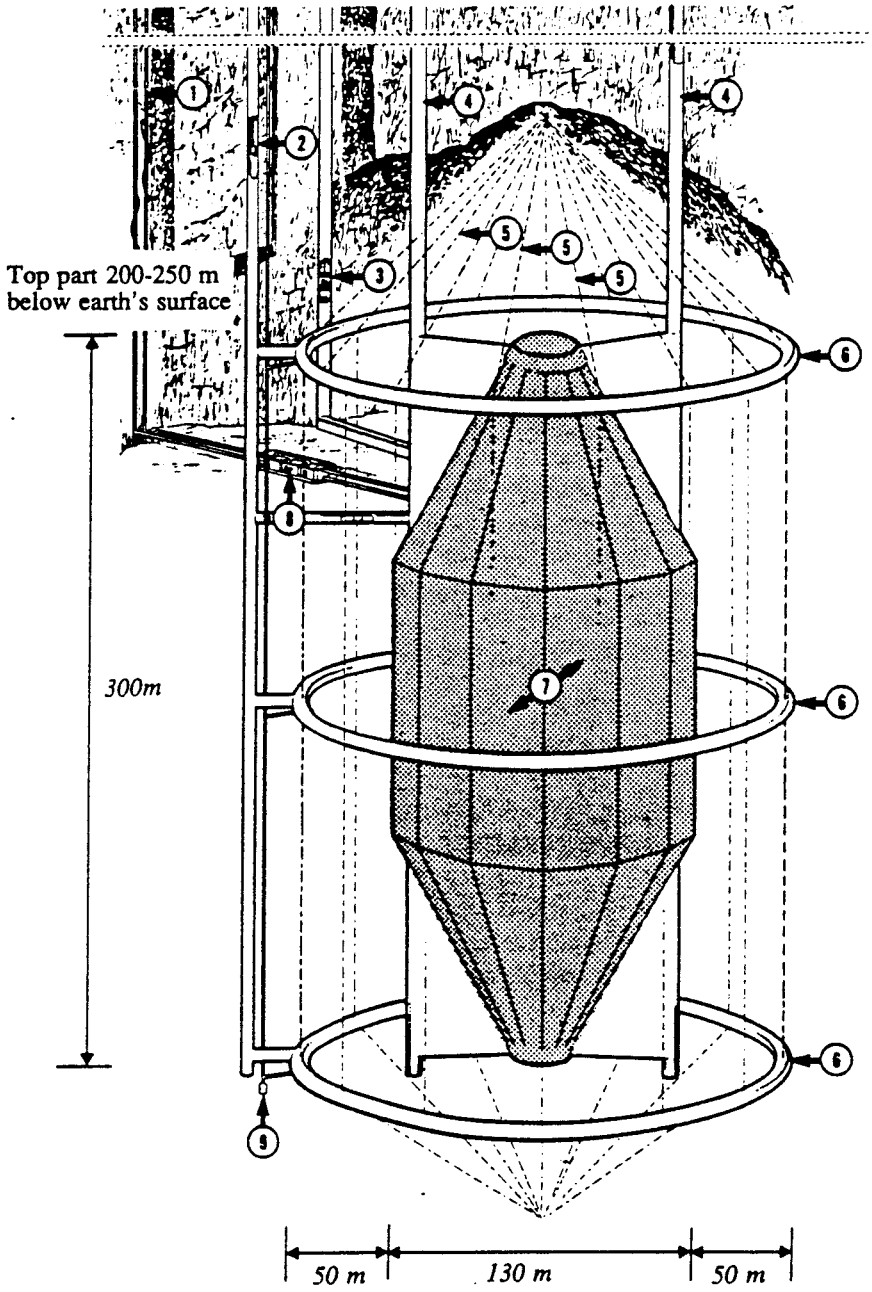

1. Ventilation shaft
2. Shaft for construction of hydraulic cage
3. Transportation of canisters
4. Main shaft for excavation and refilling of slot
5. Drillholes in hydraulic cage
6. Annular tunnels
7. Bentonite-sand barrier with a thickness of 5 m
8. Heat exchange station
9. Pump station

Figure 2-1: WP-Cave

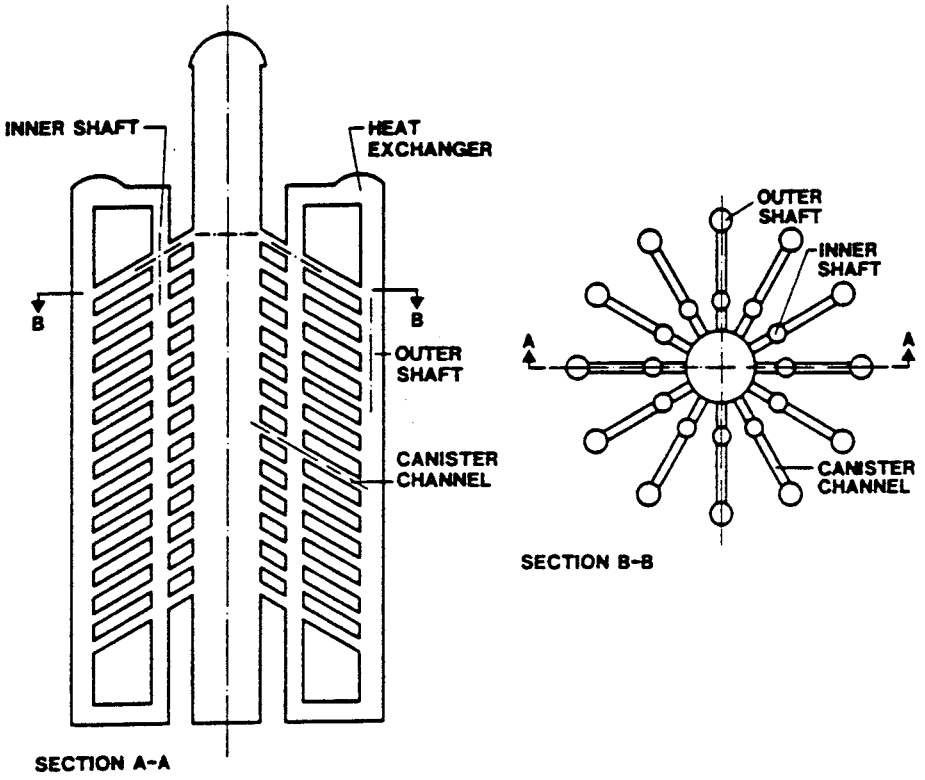

Figure 2-2: Storage layout

3. CASE DESCRIPTIONS

3.1 GENERAL

Initially, after sealing off the repository, the water in the channels and shafts is saturated with oxygen. The oxygen will cause aerobic corrosion of the steel canisters and the steel liners that covers the walls of the channels and shafts. After a time period estimated to be less than 10 years, all oxygen is consumed and anaerobic conditions are achieved. Corrosion of the canisters and repository liners will continue by direct reaction with water involving hydrogen generation and formation of divalent iron corrosion products.

Due to the high temperature maintained in the storage during several hundreds of years, the anaerobic corrosion of the steel canisters might be so fast that the canisters cannot be guaranteed to prevent water to come in contact with the fuel longer than 200 to 300 years. Once in contact with water the fuel starts to dissolve. Ionizing α-radiation from the fuel will cause radiolysis of the water near the fuel surface, resulting in a production of hydrogen and oxidants. The oxidants can react with the fuel and/or the ferrous iron present. A reaction with the fuel will transfer uranium to a higher oxidation state in which uranium is much more soluble. Oxidation of the fuel might also result in a liberation of radionuclides trapped within the uranium dioxide grains.

The dissolved nuclides will start to migrate away from the fuel surface. Redox sensitive nuclides will be reduced from a higher to a lower oxidation state by the ferrous iron during the escape through the corroded canister. For radionuclides that have a lower solubility in the reduced state, the reaction with ferrous iron may result in precipitation of the nuclide.

Once outside the canister, the nuclides will migrate through the refilled ground rock in the canister channels and enter the water flowing in fractures in the rock surrounding the channels. Due to sorption the nuclides will be retarded in the ground rock. The thermally induced water flow will transport the nuclides through the inner rock mass to the inside boundary of the bentonite-sand barrier. During this transport nuclides will sorb on the fracture surfaces. Diffusion into micro pores in the rock matrix and sorption on the micro pore surfaces will also occur. The nuclide transport out through the bentonite-sand barrier will be by advection and diffusion, influenced by sorption on the barrier material.

3.2 LOW FLOW THROUGH CASE

For the Low Flow Through Case some design parameters have been defined and some assumptions concerning the processes occurring and conditions prevailing in and around a WP-Cave repository have been made. The definitions and assumptions made are based on results from previous studies within the WP-Cave project and on advice given by the experienced members of the WP-Cave Reference Group (CARE) and the SFG-group at SKB. The design parameters relevant for the study of the nuclide release from the bentonite-sand barrier are defined as follows:

- The storage consists of a vertical central shaft with 12 radially located canister channels at 16 levels. Each canister channel passes through a vertical inner ventilation shaft and ends in a vertical outer ventilation shaft.

- The diameter of the storage is 64 m and the height is 110 m.

- The diameter of the outer ventilation shafts, inner ventilation shafts and canister channels is 3 m, 2 m and 1.7 m respectively.

- The canister channels and ventilation shafts are refilled with finely ground rock (particle size about 0.1 mm) which will prevent thermo-induced water circulation in the channels and shafts.

- The amount of concrete present in the storage is so small that the influence on the chemical environment within the storage is negligible.

- The bentonite-sand barrier is 5 m thick.

- The height of the bentonite-sand barrier is 300 m and the outer diameter is 130 m.

- The total amount of spent fuel stored in a WP-Cave is 1100 tonnes. The capacity is limited by the maximum temperature allowed near the fuel, which is 150 °C.

- The fuel is stored in steel canisters. The canisters are 5 m long and have an outer diameter of 1.3 m. Two canisters are placed in each canister channel.

The following assumptions concerning conditions and processes relevant for the radionuclide migration from the fuel to the water flowing in the rock outside the bentonite-sand barrier are made for the Low Flow Through Case.

- Because of corrosion of the steel canisters, water breakthrough occurs in all canisters after 200 years of water contact, i.e. 340 years after fuel discharge from reactor.

- Inside the canisters oxidising conditions prevail due to the radiolysis of water. Because of the iron and/or magnetite present in the storage, reducing conditions are maintained everywhere from the corroded canister walls to the rock outside the bentonite-sand barrier.

- The rate at which nuclides are released from the fuel is determined by the radiolytic oxidation of the fuel or by the solubility of the nuclide.

- 10 % of the inventory of cesium, iodine and carbon is immediately, after canister failure, released from the fuel. The release of the remaining amount is determined by the fuel oxidation rate.

- The dissolution of Ni is determined by the corrosion rate of the inconel alloy leading to an estimated dissolution time of 500 years for the total inventory of Ni.

- The corroded canisters provide no resistance to transport.

The nuclide transport from the canister surface is assumed to take place by radial diffusion through the canister channel backfilled with finely ground rock, to a fracture opening in the rock between the channels (Figure 3-1). This assumption is based on the result from a rock mechanical study where it was found that the excavation of the slot for the bentonite-sand barrier probably will open up existing fracture structures, both horizontally and vertically, in the rock mass inside the bentonite-sand barrier, with an increased hydraulic conductivity in the rock mass as a result /Håkansson et al, 1988/. This in combination with a high resistance to water flow in the channels and shafts backfilled with 0.1 mm rock particles will probably result in thermo-induced water circulation in the open fractures in the rock mass while the water in the channels and shafts remains almost stagnant. The axial diffusion in the canister channels directed towards the inner and outer ventilation shafts is neglected since the cross-sectional area available to diffusion in the axial direction is small compared to the area available to diffusion in the radial direction.

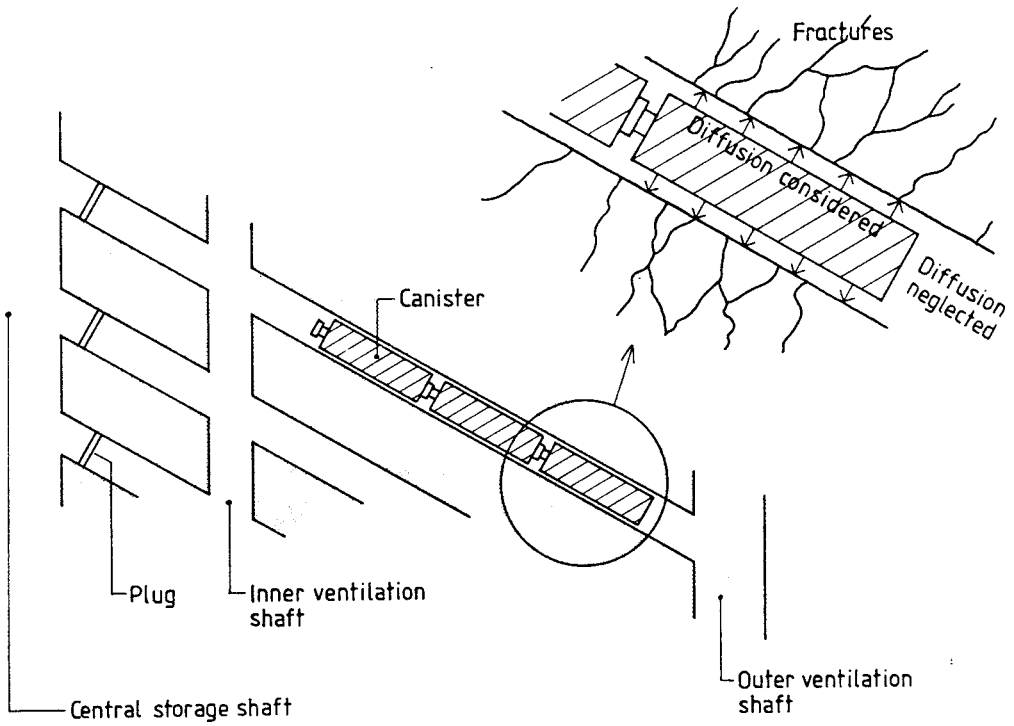

Figure 3-1: Schematic illustration of the transport in the canister channel.

The source term for the migration from the canister surface is the concentration of the nuclide in the water just outside the canister surface. The concentration at this location can never exceed the solubility of the nuclide under reducing conditions which prevail everywhere outside the canister surface. If the solubility of the nuclide is lower under oxidising than under reducing conditions, the solubility under oxidising conditions will limit the concentration just outside the canister surface. This follows from the assumption of oxidising conditions near the fuel surface. The rate with which nuclides are liberated from the fuel might, however, not be fast enough to build up the solubility concentration. In that case the concentration outside the canister surface is determined by the radiolytic fuel oxidation rate.

The increased hydraulic conductivity in the rock mass between the bentonite-sand barrier and the storage space will give a travel time for nuclides from the channel walls to the inside boundary of the bentonite-sand barrier that is estimated to be small compared to the travel times through the ground rock and the bentonite-sand barrier respectively. The transport resistance in the inner rock mass is therefore not considered, and the nuclides are assumed to enter the bentonite-sand barrier immediately after leaving the ground rock in the canister channels.

The nuclide transport through the bentonite-sand barrier will occur by advection and diffusion. The heat generated by the fuel will influence the water flow in the rock outside the barrier in such a way that inflow of water will occur through the bottom of the barrier and outflow through the top /Hopkirk, 1988/. The magnitude of the thermally induced water flow through the barrier is dependent on the hydraulic conductivities in the bentonite-sand barrier and in the internal rock mass. These hydraulic conductivities will also determine whether groundwater flow driven by the natural gradient or diffusion will be the governing transport mechanism in the bentonite-sand barrier at longer times when the temperature gradient has diminished.

In the Low Flow Through Case, the magnitude of the thermally induced flow estimated for a hydraulic conductivity of 10^{-11} m·s^{-1} in the top part and 10^{-10} m·s^{-1} in the bottom part of the bentonite-sand barrier and 10^{-9} m·s^{-1} in the inner rock mass, was applied. The transport of nuclides out through the top of the bentonite-sand barrier occurs by this thermally induced flow and diffusion acting in parallel. The thermally induced flow is, however, decreasing with time resulting in diffusion dominated release from the outer boundary of the top of the barrier at times longer than about 5000 years after canister breakthrough. The nuclide transport through the rest of the bentonite-sand barrier, and the subsequent release to the water flowing outside the barrier is assumed to be by diffusion only.

The thermo-induced flow passing along the outside of the cylindrical part of the bentonite-sand barrier is also decreasing with time. The maximum flow rate is obtained about 50 years after canister breakthrough and is approximately as high as the average natural gradient caused flow rate found in Swedish rock in site investigations at 200 metres depth. It is therefore assumed that the natural gradient determines the magnitude and direction of the water flow passing the outside of the bentonite-sand barrier at all times after canister breakthrough. The water flow rate is set to 0.3 l·m^{-2}·a^{-1} and the flow is assumed to be horizontally directed. The influence of the hydraulic cage on the water flow rate in the rock outside the barrier is not considered.

3.3 HIGH FLOW THROUGH CASE

The High Flow Through Case is the same as the Low Flow Through Case except for the nuclide transport through the bentonite-sand barrier. The difference is caused by assuming other hydraulic properties in the bentonite-sand barrier and in the inner rock mass.

It is not proven that a hydraulic conductivity of 10^{-11} m·s^{-1} can be achieved in the top part of the barrier if a low graded bentonite mixture has to be used to ascertain escape of hydrogen. A ten times higher value than that assumed in the Low Flow Through Case is possible. Also the hydraulic conductivity in the inner rock mass will probably be higher than the value assumed in the calculations of the thermally induced flow applied in the Low Flow Through Case. This is due to the large fracture apertures expected in that part of the rock /Håkansson et al, 1988/ and the higher conductivity in the backfill material in the channels and shafts.

In the High Flow Through Case a hydraulic conductivity of 10^{-10} m·s^{-1} is assumed in the bentonite-sand barrier and 10^{-7} m·s^{-1} in the inner rock mass. With these values the thermally induced water flow through the top of the barrier is calculated to be approximately 20 times higher than in the Low Flow Through Case /Hopkirk, 1988/. An illustration of the thermally induced flow in the High Flow Through Case and in the Low Flow Through Case is given in Figure 3-2. Each picture is representing the time when the flow reaches its maximum rate. The arrows show the direction of the flow and the length of the arrows is proportional to the flow rate in the actual point.

Another effect of the higher hydraulic conductivities will be an increase in the natural gradient caused water flow through the bentonite-sand barrier resulting in a nuclide release from the barrier that also at longer times is determined by flow and not, as in the Low Flow Through Case, by diffusion. Conservatively, the natural gradient caused water flow is assumed to be directed as the thermally induced water flow, i.e., vertically upwards. The nuclide transport through the top of the bentonite-sand barrier and the subsequent release occurs by advection and diffusion. The advective part is the sum of the thermally induced flow and the natural gradient driven flow. The nuclide transport through the cylindrical part is as in the Low Flow Through Case occurring by diffusion. Here, however, the nuclides are released to water flowing vertically upwards along the outside of the barrier. The magnitude of the water flow in the rock outside the bentonite-sand barrier is the same as in the Low Flow Through Case, 0.3 l·m^{-2}·a^{-1}. The presence of the hydraulic cage is not considered.

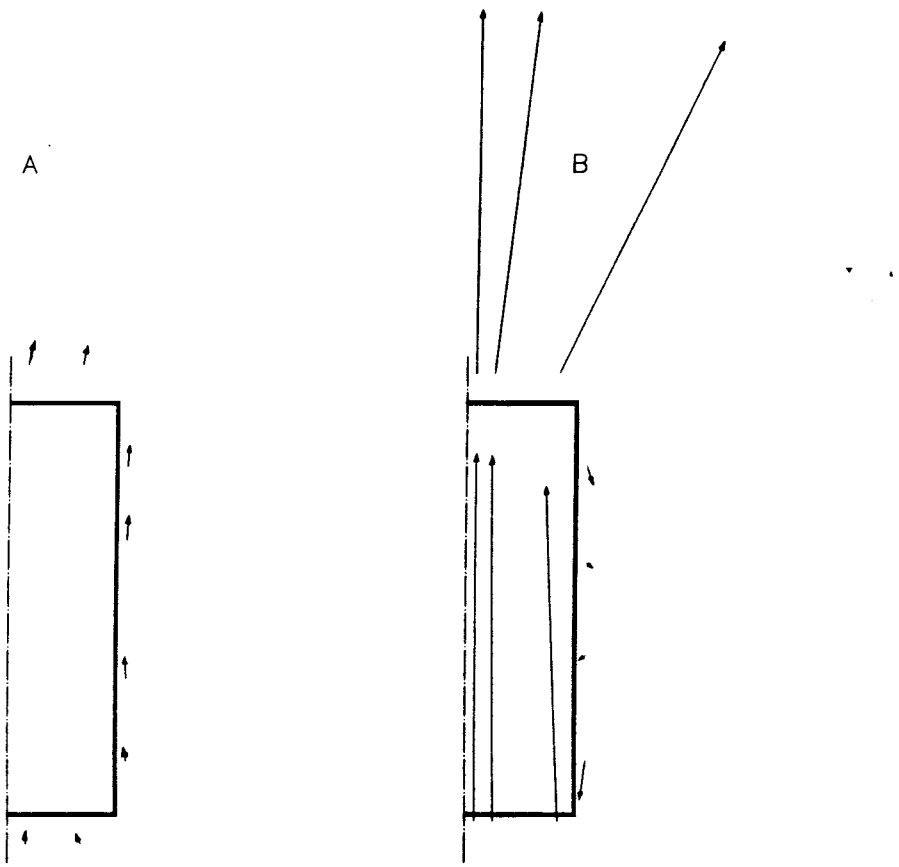

Figure 3-2: Schematic illustration of the maximum thermally induced flow in the Low Flow Through Case (A) and in the High Flow Through Case (B). (Arrow length; 1 cm = $1.1 \cdot 10^{-3}$ $m^3 \cdot m^{-2} \cdot a^{-1}$)

4. RADIONUCLIDES STUDIED

4.1 FISSION AND ACTIVATION PRODUCTS

Some of the fission and activation products will decay to an insignificant level during the transport to the rock outside the bentonite-sand barrier. These nuclides have been identified and the calculations are presented in Appendix A. In Table 4-1 the remaining fission and activation products, their half-lives and the inventory at canister breakthrough are given. The activity contribution of the individual nuclides as a function of time after canister breakthrough is shown in Figure 4-1.

Table 4-1: Fission and activation products studied.

Nuclide	Half-life (a)	Concentration in fuel 300 years after discharge from reactor	
		$g \cdot (\text{tonnes fuel})^{-1}$	$GBq \cdot (\text{tonnes fuel})^{-1}$
C-14	5 730	0.16	25.7
Ni-59	75 000	49.5	148
Se-79	65 000	6.61	17.0
Zr-93	$1.5 \cdot 10^6$	803.6	74.7
Nb-93m	*	$6.8 \cdot 10^{-3}$	71.0
Nb-94	20 000	$8.9 \cdot 10^{-4}$	0.006
Tc-99	214 000	867.8	544.6
Pd-107	$6.5 \cdot 10^6$	280.2	5.3
Sn-121m	54.9	$6.4 \cdot 10^{-5}$	0.1
Sn-126	100 000	32.1	33.7
Sb-126m	*	$1.2 \cdot 10^{-8}$	33.7
Sb-126	*	$1.5 \cdot 10^{-6}$	4.7
I-129	$16 \cdot 10^6$	206.6	1.4
Cs-135	$3 \cdot 10^6$	342.2	14.6

* Daughter in equilibrium with parent nuclide.

4.2 ACTINIDES AND DAUGHTER NUCLIDES

Some of the short lived nuclides in the beginning of the four decay chains will decay to an insignificant level before they reach the rock outside the bentonite-sand barrier. These nuclides have been identified and the calculations are presented in Appendix B. The remaining nuclides are given in Table 4-2 together with the half-lives and inventory at canister breakthrough. The activity contribution of the individual nuclides as a function of time is shown in Figure 4-2. The four decay chains are presented in Figures B1-B4 in Appendix B.

Table 4-2: Actinides and daughter nuclides studied.

Chain Nuclide	Half-life (a)	Concentration in fuel 300 years after discharge from reactor	
		g·(tonnes fuel)$^{-1}$	GBq·(tonnes fuel)$^{-1}$
4N			
Pu-240	6 570	1 615	$1.36 \cdot 10^{4}$
U-236	$23.4 \cdot 10^{6}$	4 160	10.0
Th-232	$14.1 \cdot 10^{8}$	$3.64 \cdot 10^{-2}$	$1.48 \cdot 10^{-7}$
Ra-228	*	$1.70 \cdot 10^{-11}$	$1.48 \cdot 10^{-7}$
Ac-228	*	$1.78 \cdot 10^{-15}$	$1.48 \cdot 10^{-7}$
Th-228	1.9	$2.11 \cdot 10^{-6}$	$6.39 \cdot 10^{-2}$
4N+1			
Np-237	$2.14 \cdot 10^{6}$	1 134	29.6
Pa-233	*	$3.85 \cdot 10^{-5}$	29.6
U-233	159 000	$8.10 \cdot 10^{-2}$	$2.90 \cdot 10^{-2}$
Th-229	7 300	$4.71 \cdot 10^{-5}$	$3.71 \cdot 10^{-4}$
4N+2			
Pu-242	376 000	751.1	106.2
U-238	$4.47 \cdot 10^{9}$	$9.40 \cdot 10^{5}$	11.7
Th-234	*	$1.36 \cdot 10^{-5}$	11.7
Pa-234m	*	$4.60 \cdot 10^{-10}$	11.7
U-234	245 000	361.6	83.7
Th-230	80 000	0.25	0.19
Ra-226	1 600	$2.91 \cdot 10^{-4}$	$1.06 \cdot 10^{-2}$
4N+3			
Pu-239	24 100	4 669	$1.07 \cdot 10^{4}$
U-235	$7.04 \cdot 10^{8}$	6 465	0.52
Th-231	*	$2.63 \cdot 10^{-8}$	0.52
Pa-231	32 800	$2.27 \cdot 10^{-3}$	$3.97 \cdot 10^{-3}$

* Daughter in equilibrium with parent nuclide.

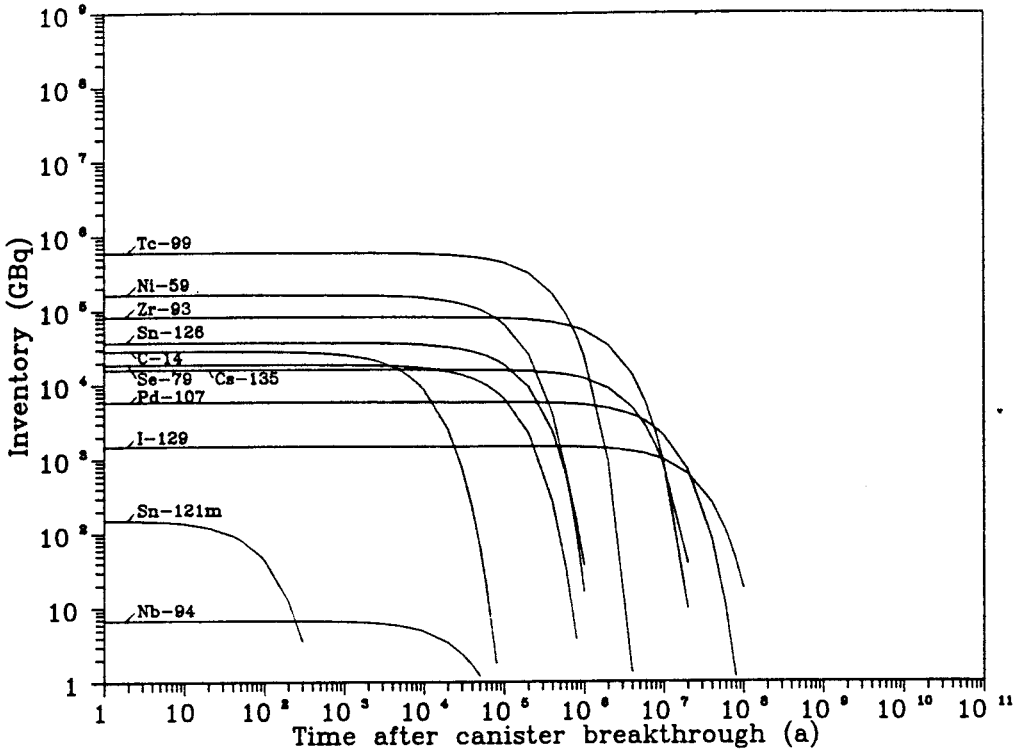

Figure 4-1: The inventory of important fission and activation products as a function of time after canister breakthrough.

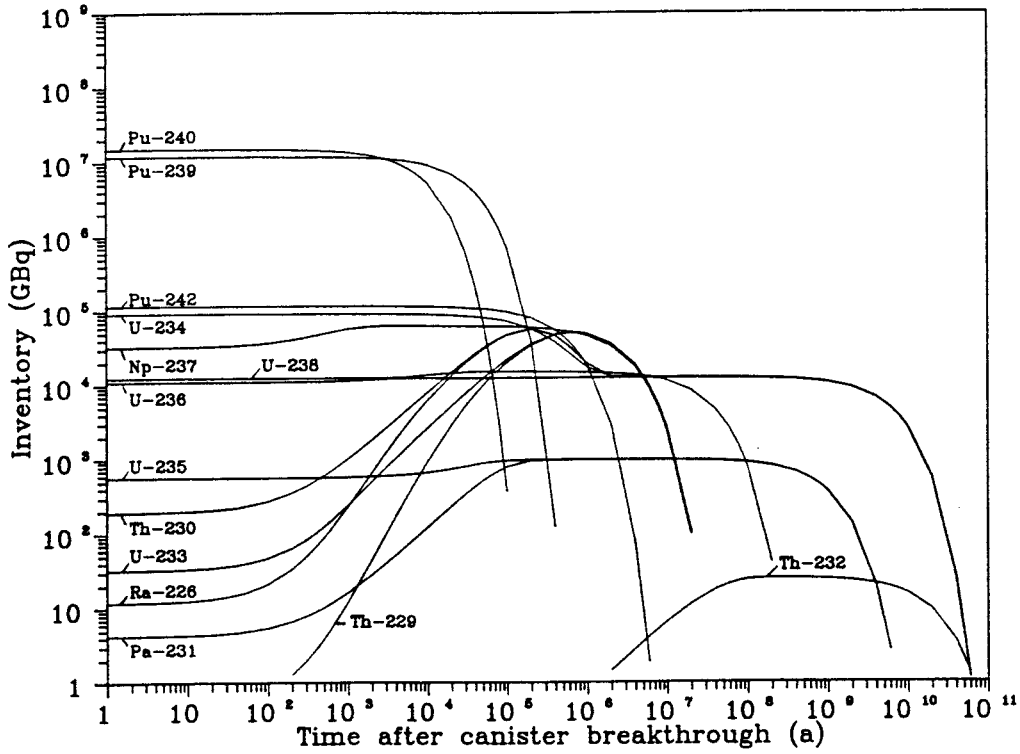

Figure 4-2: The inventory of important actinides and daughter nuclides as a function of time after canister breakthrough.

5. RELEASE CALCULATIONS

5.1 PERFORMED CALCULATIONS

5.1.1 Low Flow Through Case

The calculations performed for the Low Flow Through Case can be divided into three parts. In the first part, the nuclide release from the bentonite-sand barrier was calculated without considering any solubility limitations, i.e., the dissolution rate of each nuclide from the fuel is determined by the radiolytic fuel oxidation rate.

In the second part solubility limitations were considered. The nuclides that here are assumed to have a solubility limit are Ni, Se, Zr, Nb, Tc, Pd, Sn, Am, Pu, Np, U and Th. The concentration of these nuclides at the inlet boundary of the finely ground rock is limited by the solubility under reducing conditions. The nuclides that have a lower solubility under oxidising conditions will be limited by this solubility at the inlet of the finely ground rock. This is because the dissolution from the fuel occurs under oxidising conditions. The solubility limit on the concentration has been taken into account only at the inlet boundary of the finely ground rock. This means that the concentration of nuclides participating in chain decay might exceed the solubility during the transport through the finely ground rock and the bentonite-sand barrier.

In the third part the effect of reducing the bentonite-sand barrier from 5 m to 2.5 m has been studied. The third part also includes some calculations where the dependence of the sorption and the radiolytic fuel oxidation rate on the release from the bentonite-sand barrier has been investigated.

5.1.2 High Flow Through Case

Calculations on the High Flow Through Case were performed for some nuclides identified to be of importance to the dose to man. The nuclides studied were C-14, Se-79, Sn-126, Ni-59, I-129, Cs-135, Pu-239, Pu-240, Pu-242 and Np-237. Solubility limits were considered and treated in the same way as in the Low Flow Through Case.

5.2 MATHEMATICAL MODEL

At a time 200 years after the storage is refilled with water and finely ground rock material (340 years after fuel discharge from reactor), water penetrates the canisters and the release of nuclides from the fuel and the cladding starts. The release from the fuel is determined by the radiolytic oxidation rate or by the solubility of the nuclide. The radiolytic determined release rate of nuclide i is described by:

$$N_i(t) = \frac{F(t)}{m_F} \cdot m_i(t) \qquad (5.1)$$

where

N_i = release rate of nuclide *i* from the fuel at time t ($kg \cdot s^{-1}$)
F = radiolytic oxidation rate of the fuel at time t ($kg \cdot s^{-1}$)
m_F = initial amount of fuel (kg)
m_i = amount of nuclide *i* in the fuel at time t (kg)
t = time (s).

If nuclide *i* is the second member in a decay chain, the amount of nuclide *i* in the fuel varies with time according to:

$$m_i(t) = m_i^0 \cdot \exp(-\lambda_i t) + \frac{\lambda_{i-1} \cdot m_{i-1}^0}{\lambda_i - \lambda_{i-1}} \left[\exp(-\lambda_{i-1} t) - \exp(-\lambda_i t) \right] \qquad (5.2)$$

where

m_i^0 = initial amount of nuclide *i* in the fuel (kg)
λ_i = decay constant for nuclide *i* (s^{-1})
m_{i-1}^0 = initial amount of parent nuclide *i*-1 in the fuel (kg)
λ_{i-1} = decay constant for parent nuclide *i*-1 (s^{-1}).

For nuclides that do not participate in chain decay or are starting nuclides in decay chains, the second term on the right hand side in equation (5.2) vanishes.

The dissolved nuclide migrates through the corroded canister and enters the finely ground rock surrounding the canister. The nuclide transport through the finely ground rock in the canister channels is assumed to occur by diffusion in the radial direction. Since the thickness of the cylindrical barrier is small compared to the radius, the curvature of the finely ground rock barrier can be neglected and the transport of nuclide *i* through the barrier is given by the equation:

$$\frac{\partial c_i}{\partial t} = D_a \frac{\partial^2 c_i}{\partial z^2} - \lambda_i \cdot c_i + \lambda_{i-1} \cdot c_{i-1} \cdot \frac{\varepsilon_p + (1-\varepsilon_p) K_{i-1} \rho_s}{\varepsilon_p + (1-\varepsilon_p) K_i \rho_s} \qquad (5.3)$$

where the apparent diffusivity D_a is:

$$D_a = \frac{D_p \varepsilon_p}{\varepsilon_p + (1-\varepsilon_p) K_i \rho_s} \qquad (5.4)$$

and

c_i = liquid concentration of nuclide i ($kg \cdot m^{-3}$)
c_{i-1} = liquid concentration of parent nuclide i-1 ($kg \cdot m^{-3}$)
K_i = sorption coefficient for nuclide i ($m^3 \cdot kg^{-1}$)
K_{i-1} = sorption coefficient for parent nuclide i-1 ($m^3 \cdot kg^{-1}$)
D_p = diffusivity of nuclide i in pore liquid ($m^2 \cdot s^{-1}$)
z = length coordinate in the diffusion direction (m)
ε_p = porosity of the barrier ($m^3 \cdot m^{-3}$)
ρ_s = solid density of the barrier material ($kg \cdot m^{-3}$).

The initial condition is:

$$c_i = c_{i-1} = 0 \quad \text{for} \quad z > 0 \quad \text{at } t = 0 \tag{5.5}$$

Since the transport resistance in the corroded canister is not considered, the boundary condition at the inlet of the finely ground rock barrier, z = 0, for t > 0 becomes:

$$N_i(t) = -(D_p \varepsilon_p A)_r \cdot \left. \frac{dc_i}{dz} \right|_{z=0} \tag{5.6}$$

where subscript r refers to the finely ground rock barrier and A is the cross sectional area available for diffusion. Some nuclides may have such low solubility that they precipitate before entering the finely ground rock barrier. For these nuclides the boundary condition at z = 0 becomes:

$$c_i = c_{i,sol} \qquad \text{for } t > 0 \tag{5.7}$$

The nuclide transport through the top of the barrier occurs by diffusion and advection acting in parallel, and is described by:

$$\frac{\partial c_i}{\partial t} = D_a \frac{\partial^2 c_i}{\partial z^2} - \frac{v}{R} \cdot \frac{\partial c_i}{\partial z} - \lambda_i c_i + \lambda_{i-1} c_{i-1} \cdot \frac{\varepsilon_p + (1-\varepsilon_p) K_{i-1} \rho_s}{\varepsilon_p + (1-\varepsilon_p) K_i \rho_s} \tag{5.8}$$

where the retardation factor R is defined as:

$$R = \frac{\varepsilon_p + (1-\varepsilon_p) K_i \rho_s}{\varepsilon_p} \qquad (5.9)$$

and v is the water velocity ($m \cdot s^{-1}$) in the barrier. The water velocity is determined by the thermo-induced flow in the Low Flow Through Case and by the sum of the thermo-induced flow and the natural gradient driven flow in the High Flow Through Case. The nuclide transport out through the other parts of the bentonite-sand barrier is given by equation (5.3), the diffusion equation.

Since the transport resistance in the rock between the finely ground rock barrier and the bentonite-sand barrier is neglected, all nuclides escaping from the finely ground rock barrier enters the bentonite-sand barrier. The boundary condition at the inlet of the bentonite-sand barrier, $z = z_1$, for $t > 0$ is then given by:

$$\left[-D_p \varepsilon_p A \cdot \frac{dc_i}{dz}\bigg|_{z=z_1}\right]_r = \left[-D_p \varepsilon_p A \cdot \frac{dc_i}{dz}\bigg|_{z=z_1} + v \cdot \varepsilon_p \cdot A \cdot c_i(z_1)\right]_T +$$

$$+ \left[-D_p \varepsilon_p A \cdot \frac{dc_i}{dz}\bigg|_{z=z_1}\right]_b \qquad (5.10)$$

where subscript r refers to the finely ground rock, T to the top part of the bentonite-sand barrier and b to the remaining part of the bentonite-sand barrier where transport out of nuclides occurs.

In the Low Flow Through Case it is assumed that nuclides are escaping by diffusion not only through the cylindrical part but also through the bottom of the bentonite-sand barrier. The diffusion out through the bottom part will during the early time period be hindered by the opposite directed thermo-induced inflow of water. This has, however, been neglected. In the High Flow Through Case the inflow of water through the bottom of the bentonite-sand barrier will all the time counteract any transport out of nuclides through this part of the barrier. It has therefore been assumed that no nuclide transport will occur through the bottom part of the bentonite-sand barrier in this case.

The boundary condition at the outlet of the cylindrical part and, in the Low Flow Through Case, the bottom part of the bentonite-sand barrier, $z = z_2$, is given by:

$$N'_i = -D_p \varepsilon_p A' \cdot \frac{dc_i}{dz}\bigg|_{z=z_2} = Q'_{eq} \cdot c'_i(z_2) \qquad (5.11)$$

where

$$Q'_{eq} = A' \cdot \varepsilon_f \cdot \left[\frac{4 \cdot D_v \cdot u_o}{\pi \cdot L' \cdot \varepsilon_f} \right]^{1/2} \qquad (5.12)$$

and

$c'_i(z_2)$ = concentration of nuclide i at the outlet boundary of the cylindrical (and bottom) part of the barrier, $(kg \cdot m^{-3})$

N'_i = release rate of nuclide i from the cylindrical (and bottom) part of the barrier, $(kg \cdot s^{-1})$

A' = total outer surface of the cylindrical (and bottom) part of the barrier, (m^2)

ε_f = flow porosity in the rock outside the barrier, $(m^3 \cdot m^{-3})$

D_v = nuclide diffusivity in bulk water, $(m^2 \cdot s^{-1})$

u_o = water flow rate in the rock outside the barrier, $(m^3 \cdot m^{-2} \cdot s^{-1})$

L' = length of the water flow path outside the cylindrical (and bottom) part of the barrier, (m).

The release rate at the outlet boundary of the top of the bentonite-sand barrier in the Low Flow Through Case is described by:

$$N_i^T = -(D_p \varepsilon_p A)_T \cdot \frac{dc_i}{dz}\bigg|_{z=z_2} + v \cdot \varepsilon_p A_T \cdot c_i(z_2) =$$

$$= (v \cdot \varepsilon_p \cdot A_T + Q_{eq}^T) \cdot c_i(z_2) \qquad (5.13)$$

where

$$Q_{eq}^T = A_T \cdot \varepsilon_f \cdot \left[\frac{4 \cdot D_v \cdot u_o}{\pi \cdot L_T \cdot \varepsilon_f} \right]^{1/2} \qquad (5.14)$$

and

N_i^T = release rate of nuclide i from the top of the barrier, $(kg \cdot s^{-1})$

$c_i(z_2)$ = concentration of nuclide i at the outlet boundary of the top of the barrier, $(kg \cdot m^{-3})$

A_T = area of the top of the barrier, (m^2)

L_T = length of the water flow path outside the top, (m).

The above boundary condition states that the total release from the top of the barrier is the sum of the release by the thermo-induced flow and by diffusion.

The release by diffusion is expressed in analogy with the release by diffusion from the bottom and cylindrical parts of the barrier, i.e., the driving force for the diffusional transport is assumed to be the concentration difference between the outlet boundary of the barrier and the water flowing horizontally along this part of the barrier. Eventually, this diffusional transport will totally dominate the release from the barrier since the thermo-induced flow through the top of the barrier is decreasing with time.

In the High Flow Through Case the natural gradient induced water flow is assumed to be vertically directed. The water flow through the top is therefore composed of both the natural gradient flow and the thermo-induced flow. The release rate at the outlet boundary of the top of the bentonite-sand barrier by diffusion will in this case be very small compared to the release by flow, at all times. The diffusion term in equation (5.13) is therefore omitted in the High Flow Through Case calculations.

5.3 CALCULATION MODEL AND DATA USED

The multi-dimensional integrated finite difference codes TRUMP /Edwards, 1972/ and TRUCHN, a modified version of TRUMP which can handle decay chains, were used to solve the transport equations. The nuclide migration was modelled as one-dimensional transport through two flat barriers in series, with two parallel pathways through the second barrier. This simplification was made since the design of a WP-Cave is symmetric and the curvature of the ground rock barrier and the bentonite-sand barrier can be neglected. The mesh geometries used in the Low Flow Through Case and the High Flow Through Case, with indicated nodal points, transport lengths and areas, are shown in Figure 5-1 and 5-2, respectively.

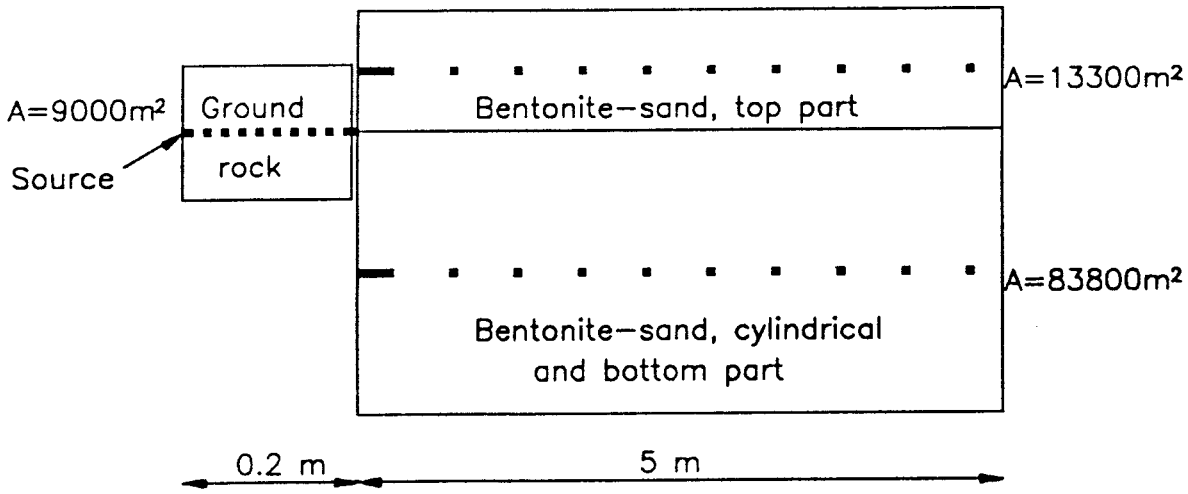

Figure 5-1: Mesh geometry used in the Low Flow Through Case calculations.

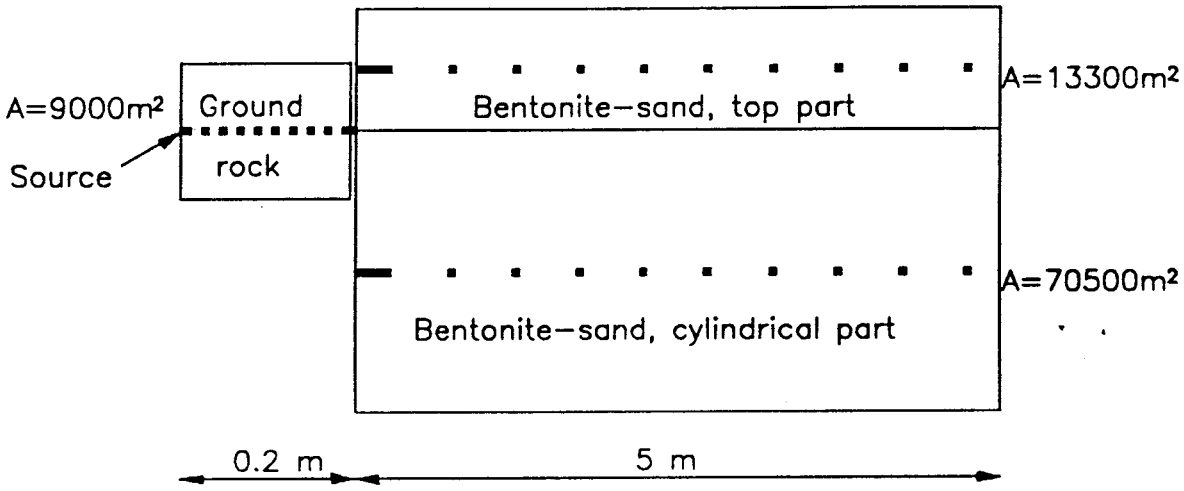

Figure 5-2: Mesh geometry used in the High Flow Through Case calculations.

The radiolytic fuel oxidation rate used in the calculations is shown in Figure 5-3. After $1.2 \cdot 10^6$ years, all fuel in the storage, 1100 tons, is oxidised. The initial rate has been conservatively estimated /Werme, 1988/ from experimental data and theoretical calculations /Christensen and Bjergbakke, 1987/.

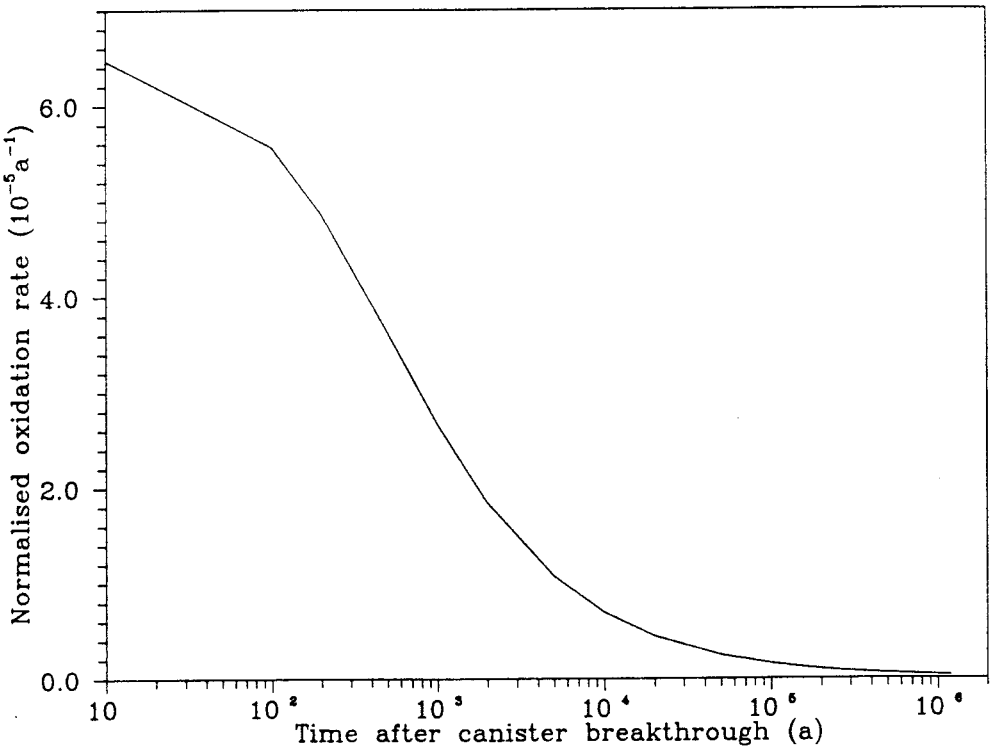

Figure 5-3: Normalised radiolytic fuel oxidation rate.

The total water flow through the top part of the bentonite-sand barrier versus time after canister breakthrough in the Low Flow Through Case and in the High Flow Through Case is shown in Figure 5-4. Values of the thermally induced flow up to 3000 years after canister breakthrough are from Hopkirk /1988/. At times longer than 3000 years, the thermally induced flow rate is decreased in proportion to the decrease in thermal power in the fuel. The curve for the High Flow Through Case is the sum of the thermally induced and the natural gradient flow. The natural flow through the repository is assumed to be constant in time and has been estimated to 11 $m^3 \cdot a^{-1}$ (see Appendix C).

The material properties of the finely ground rock barrier and the bentonite-sand barrier are given in Table 5-1. Sorption and diffusivity data for the nuclides in the finely ground rock are presented in Table 5-2. Values representative at room temperature were used because data on sorption at temperatures as high as 150 °C are limited. For Pd, Sn and U, additional calculations with a more conservative sorption value have been made. Both the conservative and the central values are given in Table 5-2.

Due to lack of data on sorption in bentonite-sand mixtures under reducing conditions, the data used in the SFR-study on sorption and diffusion in 10/90 bentonite-sand mixtures under oxidising conditions were also applied in this study (Table 5-3). Reducing conditions will result in higher sorption coefficients for the redox sensitive Tc, Pu, Np and U, and values given by B. Allard (personal communication) are included in the table. As a variation, the effect of the higher sorption values for Np and U has been determined for one of the decay chains. Also the effect of no sorption of Pd and Sn in the bentonite-sand barrier has been studied.

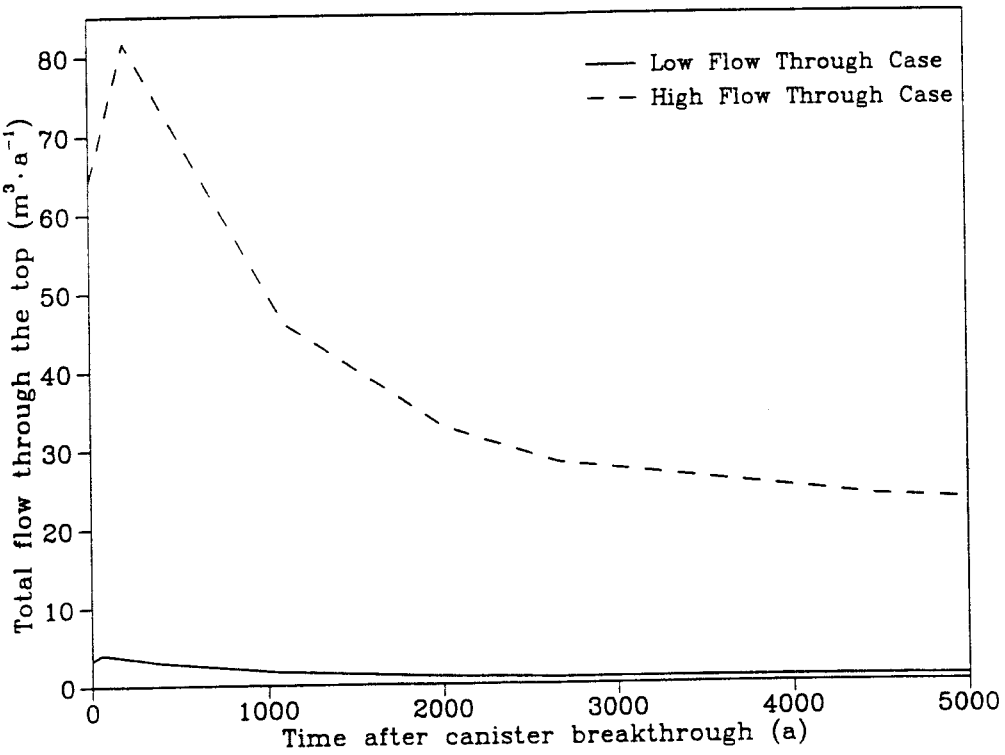

Figure 5-4: Total water flow through the top of the barrier.

The convective boundary condition at the outlet of the bentonite-sand barrier (eq. 5.11 and 5.13) includes the equivalent water flow Q'_{eq} and Q^{T}_{eq}. The equivalent water flow calculated from equations (5.12) and (5.14), and the data used in the calculation are given in Table 5-4.

In Table 5-5 the solubilities used in the calculations are presented for those elements which here are assumed to have a solubility limit. Due to the very limited amount of thermodynamic data at temperatures up to 150 °C, solubilities at room temperature were used in the calculations. The solubility applied for Nb is the concentration in equilibrium with solid $Ca(NbO_3)_2$. Under prevailing conditions it is more likely that the solid phase is Nb_2O_5 which have a considerably lower solubility (I. Grenthe, personal communication). The solubility used for Pd pressumes PdO as the solid phase. If instead solid $Pd(OH)_2$ determines the concentration, a higher solubility than the value given in Table 5-5 should be applied.

For all elements, except Pu, the solubility under reducing conditions is lower than under oxidising conditions and will therefore limit the concentration at the inlet boundary of the finely ground rock. This is based on the assumption that the canister corrosion will maintain reducing conditions at the boundary between the canisters and the finely ground rock. Due to the radiolysis of water near the fuel the dissolution of the fuel will occur under oxidising conditions. The concentration of Pu at the inlet boundary of the finely ground rock will thus be limited by the solubility under oxidising conditions.

The solubility of each element given in Table 5-5 is the sum of the concentrations of all isotopes of that element. The solubility of each isotope of an element at different times has been determined by proportioning the solubility in Table 5-5 with the relative amount of the isotope in the inventory at the actual time.

Table 5-1: Material properties.

	Finely ground rock	Bentonite-sand (10/90)
Total area, (m^2)	9 000	97 000
Top/bottom part		13 300
Cylindrical part		70 500
Thickness, (m)	0.20	5
Porosity	0.30	0.25
Density (solid), ($kg \cdot m^{-3}$)	2 700	2 666
Density (bulk), ($kg \cdot m^{-3}$)	1 890	2 000

Table 5-2: Sorption and diffusivity data, finely ground rock. Room temperature and reducing conditions. $D_p = 2 \cdot 10^{-9}\ m^2 \cdot s^{-1}$.

Specie	K_d ($m^3 \cdot kg^{-1}$)	Ref	K_d used ($m^3 \cdot kg^{-1}$)	D_a from eq.5.4 ($m^2 \cdot s^{-1}$)
C	0 – 0.005	(a)	0	$2.0 \cdot 10^{-9}$
Ni	0.005 – 0.2	(a)	0.2	$1.6 \cdot 10^{-12}$
	0.2	(b)		
Se	0 – 0.005	(a)	0.001	$2.7 \cdot 10^{-10}$
Zr	0.1 – 5	(a)	4	$7.9 \cdot 10^{-14}$
	4	(b)		
Nb	0.1 – 0.5	(c)	4	$7.9 \cdot 10^{-14}$
	4	(b)		
Tc	0.005 – 0.25	(a)	0.05	$6.3 \cdot 10^{-12}$
	0.005 – 0.05	(c)		
	0.05	(b)		
Pd	0 – 0.01	(a)	0.001	$2.7 \cdot 10^{-10}$
	0 – 0.01	(c)	(0)	$2.0 \cdot 10^{-9}$
Sn	0 – 0.05	(a)	0.001	$2.7 \cdot 10^{-10}$
	0 – 0.1	(c)	(0)	$2.0 \cdot 10^{-9}$
I	0 – 0.001	(a)	0	$2.0 \cdot 10^{-9}$
	0	(b)		
Cs	0.05 – 0.25	(a)	0.05	$6.3 \cdot 10^{-12}$
	0.05	(b)		
Am	0.5 – 5	(a)	5	$6.3 \cdot 10^{-14}$
	5	(b)		
Pu	0.5 – 5	(a)	5	$6.3 \cdot 10^{-14}$
	5	(b)		
Np	0.1 – 1	(a)	5	$6.3 \cdot 10^{-14}$
	5	(b)		
U	0.05 – 1	(a)	5	$6.3 \cdot 10^{-14}$
	5	(b)	(1)	$3.2 \cdot 10^{-13}$
Pa	0.01 – 1	(a)	5	$6.3 \cdot 10^{-14}$
	5	(b)		
Th	0.01 – 1	(a)	5	$6.3 \cdot 10^{-14}$
	5	(b)		
Ra	0.05 – 1	(a)	0.1	$3.2 \cdot 10^{-12}$
	0.1	(b)		

(a) McKinley and Hadermann, 1985
(b) Allard et al, 1985
(c) KBS-3, 1983

( ) value used in variation calculation

Table 5-3: Sorption and diffusivity data, 10/90 bentonite-sand. Room temperature and oxidising conditions. $D_p = 4 \cdot 10^{-10}\ m^2 \cdot s^{-1}$ *(d).*

Specie	K_d ($m^3 \cdot kg^{-1}$)	Ref	D_a from eq.5.4 ($m^2 \cdot s^{-1}$)	Comments
C	0	(d)	$4.0 \cdot 10^{-10}$	
Ni	0.025	(d)	$2.0 \cdot 10^{-12}$	
Se	0.0003		$1.6 \cdot 10^{-11}$	same as I^- assumed
Zr	0.4	(d)	$1.2 \cdot 10^{-13}$	
Nb	0.1	(d)	$5.0 \cdot 10^{-13}$	
Tc	0.0005	(d)	$9.8 \cdot 10^{-12}$	
	0.1	(e)	$5.0 \cdot 10^{-13}$	reducing condition
Pd	0.0005	(e)	$9.8 \cdot 10^{-12}$	same as Tc assumed
	0		$1.0 \cdot 10^{-10}$	conservative value
Sn	0.0005	(e)	$9.8 \cdot 10^{-12}$	same as Tc assumed
	0		$1.0 \cdot 10^{-10}$	conservative value
I	0.0003	(d)	$1.6 \cdot 10^{-11}$	
Cs	0.025	(d)	$4.5 \cdot 10^{-12}$	D_a from (d)
Am	1.26	(d)	$4.0 \cdot 10^{-14}$	
Pu	0.1	(d)	$5.0 \cdot 10^{-13}$	
	0.3	(e)	$1.7 \cdot 10^{-13}$	reducing condition
Np	0.013	(d)	$3.8 \cdot 10^{-12}$	
	0.3	(e)	$1.7 \cdot 10^{-13}$	reducing condition
U	0.006	(f)	$8.2 \cdot 10^{-12}$	
	0.3	(e)	$1.7 \cdot 10^{-13}$	reducing condition
Pa	0.3		$1.7 \cdot 10^{-13}$	same as Th assumed
Th	0.3	(d)	$1.7 \cdot 10^{-13}$	
Ra	0.09	(d)	$5.6 \cdot 10^{-13}$	

(d) Wiborgh and Lindgren, 1987
(e) Allard, personal communication, 1988
(f) Allard et al, 1978

Table 5-4: Equivalent water flows and data used to calculate them.

Water flow rate in the rock outside the bentonite-sand barrier	$0.3 \cdot 10^{-3}$ $m^3 \cdot m^{-2} \cdot a^{-1}$
Flow porosity in the rock outside the bentonite-sand barrier	$1 \cdot 10^{-3}$ $m^3 \cdot m^{-3}$
Nuclide diffusivity in water	$2 \cdot 10^{-9}$ $m^2 \cdot s^{-1}$
Length of water flow path on the outside of the bentonite-sand barrier:	
Low Flow Through Case, horizontal flow;	
Top part	130 m
Bottom and cylindrical part	200 m
High Flow Through Case, vertical flow;	
Cylindrical part	210 m
Calculated equivalent water flow:	
Low Flow Through Case, Q^T_{eq}	0.18 $m^3 \cdot a^{-1}$
Low Flow Through Case, Q'_{eq}	0.91 $m^3 \cdot a^{-1}$
High Flow Through Case, Q'_{eq}	0.75 $m^3 \cdot a^{-1}$

Table 5-5: Solubilities used in the calculations. Reducing conditions, room temperature and neutral pH.

Element	Solubility $kg \cdot m^{-3}$	Reference
Ni	$6 \cdot 10^{-3}$	Neretnieks and Andersson, 1978
Se	$8 \cdot 10^{-5}$	Karlsson, Höglund, Pers, 1986
Zr	$9 \cdot 10^{-9}$	Baes, Mesmer, 1976
Nb	$1 \cdot 10^{-4}$	Andersson, Torstenfelt, Rydberg, 1979
Tc	$2 \cdot 10^{-7}$	KBS-3, 1983
Pd	$2 \cdot 10^{-8}$	Karlsson, Höglund, Pers, 1986
Sn	$1 \cdot 10^{-4}$	Karlsson, Höglund, Pers, 1986
Am	$6 \cdot 10^{-3}$	KBS-3, 1983
Pu	$8 \cdot 10^{-6}$*	KBS-3, 1983
Np	$8 \cdot 10^{-6}$	KBS-3, 1983
U	$1 \cdot 10^{-5}$	KBS-3, 1983
Th	$4 \cdot 10^{-7}$	KBS-3, 1983

* oxidising conditions.

6. RESULTS

6.1 LOW FLOW THROUGH CASE

6.1.1 Solubility limitations not considered

The release rate from the bentonite-sand barrier versus time after canister breakthrough for the fission and activation products is shown in Figure 6-1, and for the nuclides in the four decay chains in Figures 6-2 to 6-5. A presentation of the four decay chains is given in Appendix B, Figures B1-B4. In Figure 6-6, the release rates of the actinides and daughters in the decay chains are put together in one graph. The maximum release rate of each nuclide and the time when the maximum release rate is obtained is given in Table 6-1.

When solubility limits are not considered, C-14 and Tc-99 will dominate the release of fission and activation products (Figure 6-1). The maximum release rate of C-14 is obtained as early as 600 years after canister breakthrough. The early release and the high maximum release rate is mainly the result of no sorption in the barriers. The high maximum release rate of Tc-99 is explained by low sorption, especially in the bentonite-sand, in combination with high initial amount in the fuel and relatively long half-life.

Among the nuclides in the four decay chains, the uranium isotopes and Np-237 will dominate the release rate from the bentonite-sand barrier (Figure 6-6). This is also the result of a combination of low sorption in the bentonite-sand, high initial amount in the fuel and long half-lives.

In Figure 6-7 the release rates of the dominating nuclides are shown. The release of fission and activation products occurs earlier in time than the release of actinides and daughters. The level of the release rate of fission and activation products is also markedly higher.

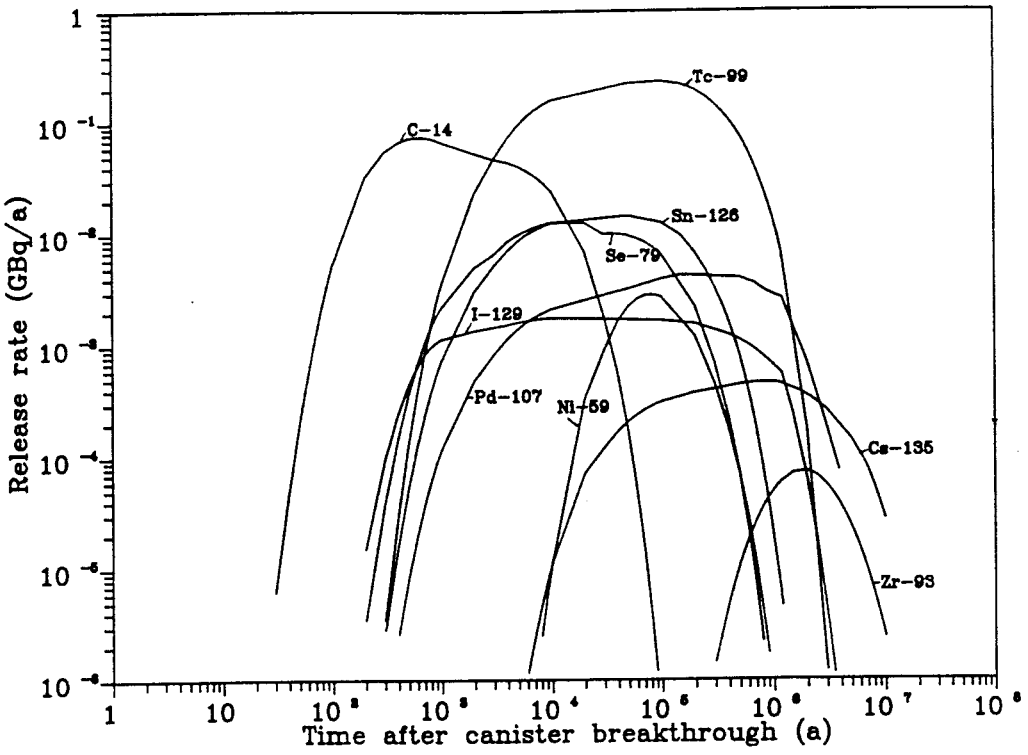

Figure 6-1: Release rates of fission and activation products from the bentonite-sand barrier versus time after canister breakthrough. Solubility limitations are not considered.

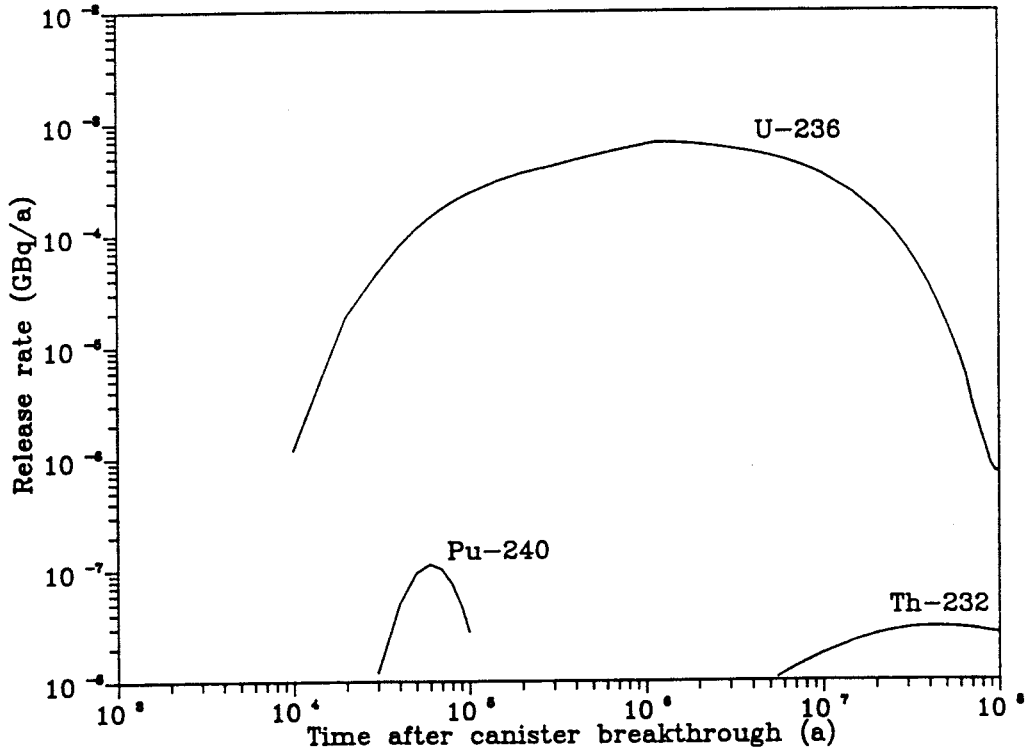

Figure 6-2: Release rates from the bentonite-sand barrier of nuclides in Chain 4N versus time after canister breakthrough. Solubility limitations are not considered.

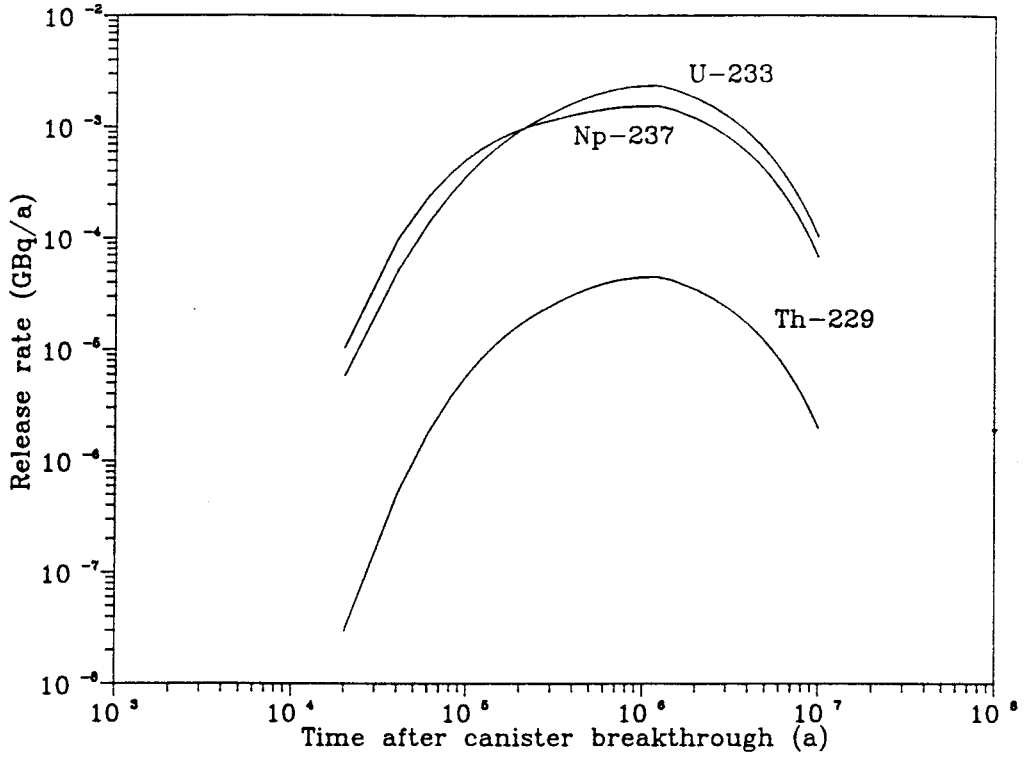

Figure 6-3: Release rates from the bentonite-sand barrier of nuclides in Chain 4N+1 versus time after canister breakthrough. Solubility limitations are not considered.

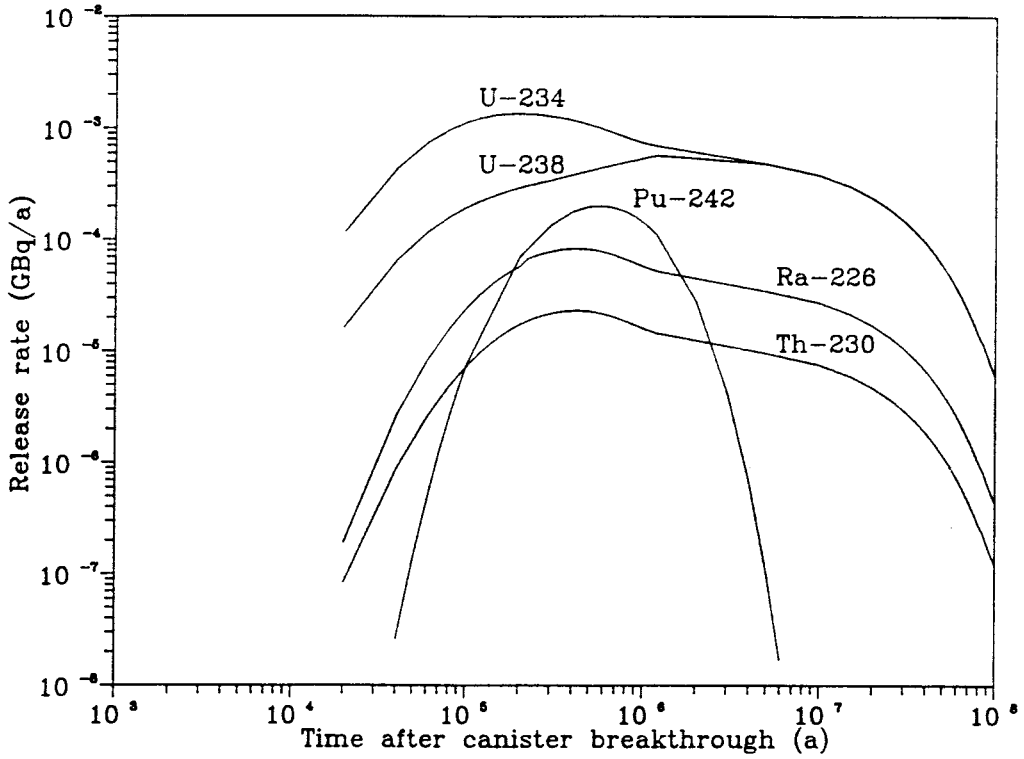

Figure 6-4: Release rates from the bentonite-sand barrier of nuclides in Chain 4N+2 versus time after canister breakthrough. Solubility limitations are not considered.

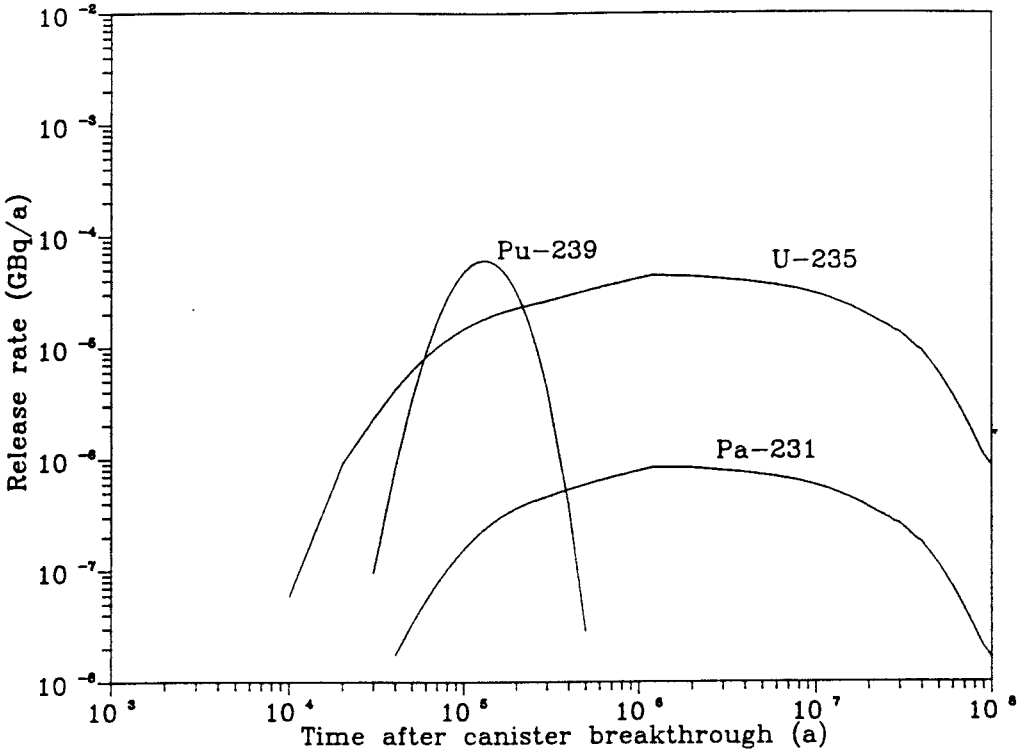

Figure 6-5: Release rates from the bentonite-sand barrier of nuclides in Chain 4N+3 versus time after canister breakthrough. Solubility limitations are not considered.

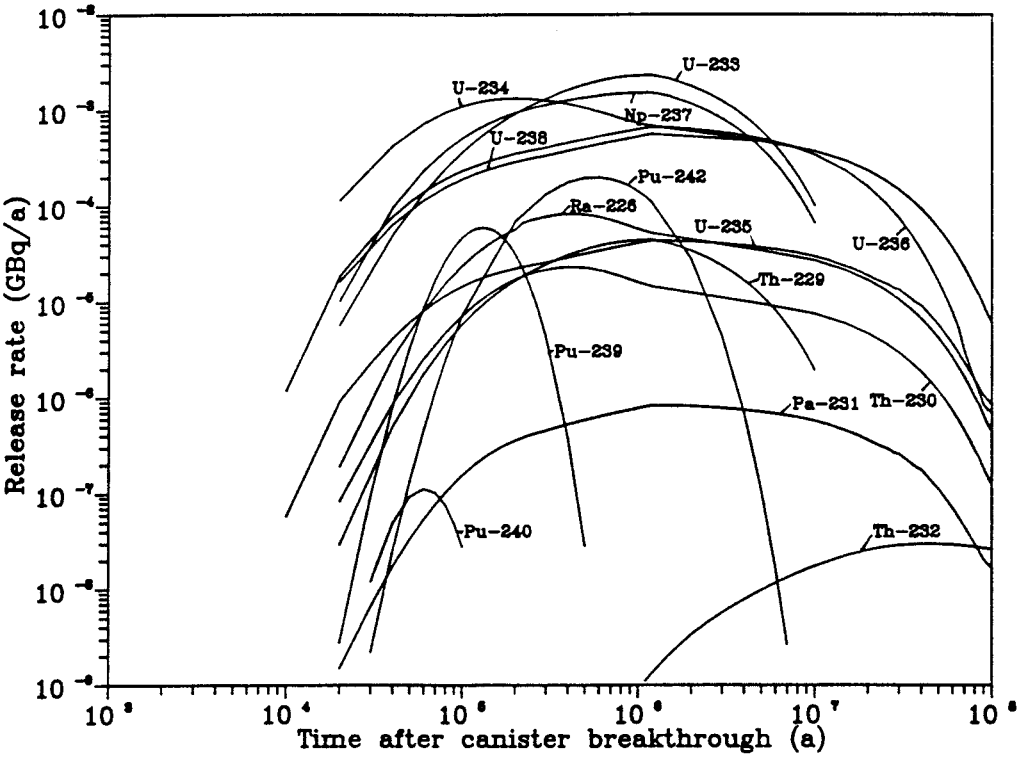

Figure 6-6: Release rates of actinides and daughters from the bentonite-sand barrier versus time after canister breakthrough. Solubility limitations are not considered.

Table 6-1: Maximum release rate and corresponding time. Solubility limitations are not considered.

Nuclide	Maximum release rate, ($GBq \cdot a^{-1}$)	Time after canister breakthrough, (a)
C-14	$7.4 \cdot 10^{-2}$	600
Ni-59	$2.8 \cdot 10^{-3}$	80 000
Se-79	$1.3 \cdot 10^{-2}$	10 000
Zr-93	$6.0 \cdot 10^{-3}$	$1.2 \cdot 10^{6}$
Nb-94	$1.9 \cdot 10^{-11}$	100 000
Tc-99	$2.3 \cdot 10^{-1}$	100 000
Pd-107	$4.2 \cdot 10^{-3}$	150 000
Sn-121m	$4.4 \cdot 10^{-10}$	400
Sn-126	$1.4 \cdot 10^{-2}$	50 000
I-129	$1.8 \cdot 10^{-3}$	10 000
Cs-135	$4.6 \cdot 10^{-4}$	800 000
Ra-226	$8.3 \cdot 10^{-5}$	420 000
Th-229	$4.5 \cdot 10^{-5}$	$1.2 \cdot 10^{6}$
Th-230	$2.3 \cdot 10^{-5}$	420 000
Th-232	$3.0 \cdot 10^{-8}$	$4.5 \cdot 10^{7}$
Pa-231	$8.3 \cdot 10^{-7}$	$1.2 \cdot 10^{6}$
U-233	$2.3 \cdot 10^{-3}$	$1.2 \cdot 10^{6}$
U-234	$1.3 \cdot 10^{-3}$	200 000
U-235	$4.4 \cdot 10^{-5}$	$1.2 \cdot 10^{6}$
U-236	$6.7 \cdot 10^{-4}$	$1.2 \cdot 10^{6}$
U-238	$5.7 \cdot 10^{-4}$	$1.2 \cdot 10^{6}$
Np-237	$1.5 \cdot 10^{-3}$	$1.2 \cdot 10^{6}$
Pu-239	$6.0 \cdot 10^{-5}$	130 000
Pu-240	$1.1 \cdot 10^{-7}$	60 000
Pu-242	$2.0 \cdot 10^{-4}$	600 000

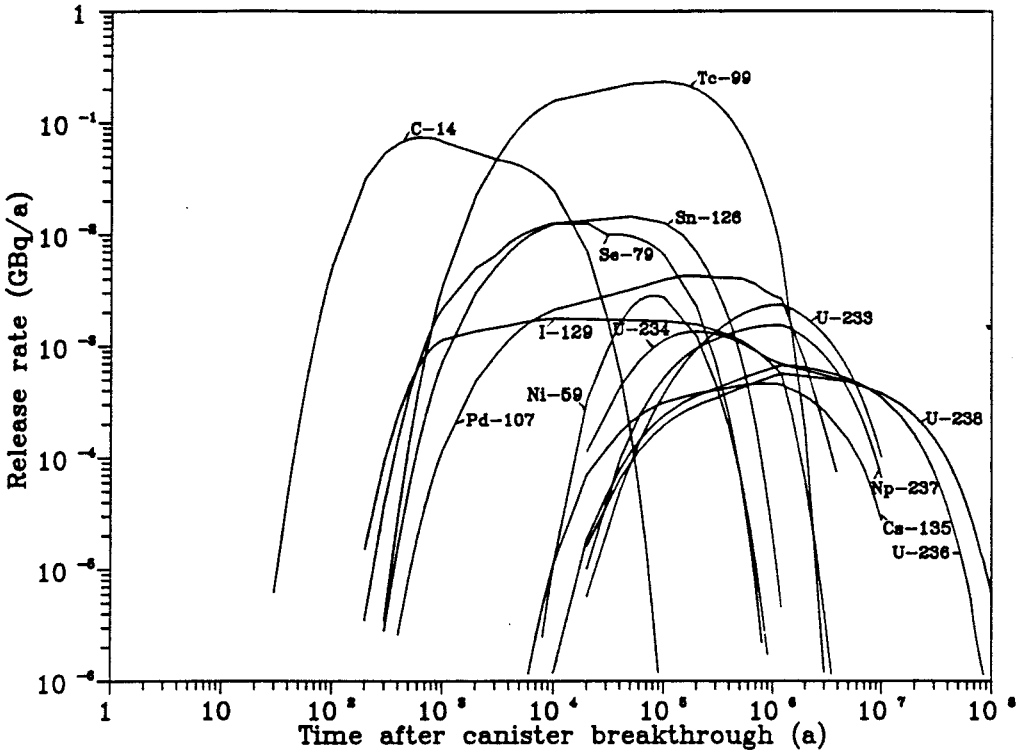

Figure 6-7: Release rates of dominating nuclides from the bentonite-sand barrier versus time after canister breakthrough. Solubility limitations are not considered.

6.1.2 Solubility limitations considered

The radiolytic fuel oxidation rate will, for many of the nuclides, result in a concentration at the inlet of the finely ground rock barrier which exceeds the solubility. Therefore, in the second set of calculations, the concentration of these nuclides at the inlet of the finely ground rock barrier was set to the solubility.

The release rates of the fission and activation products are given in Figure 6-8, and of the nuclides in the four decay chains in Figures 6-9 to 6-12. The results for the actinides and daughter nuclides in the decay chains are compiled in Figure 6-13. The maximum release rate of the solubility limited nuclides and corresponding time are given in Table 6-2 together with the ratio of the maximum release rates obtained without and with considering solubility limitations.

Among the fission and activation products, Tc-99 and Pd-107 will be solubility limited using the solubilities given in Table 5-5. Because of the solubility limit, the release rate of these two nuclides will be considerable lower than shown earlier in Figure 6-1, and Tc-99 will no longer be one of the dominating nuclides (Figure 6-8 and Table 6-2).

The nuclides in Chain 4N (Pu-240 → U-236 → Th-232) will all be solubility limited at the inlet of the finely ground rock. Taking this into account will result in lower release rates, especially for U-236 (Figure 6-9, Figure 6-2 and Table 6-2). The first peak on the U-236 curve is obtained because the concentration of U-236 in the barriers exceeds the solubility during that period (only the concentration at the inlet boundary of the finely ground rock is limited in the calculations). The higher concentration of U-236 in the barriers compared to the concentration at the inlet of the finely ground rock is caused by decay of Pu-240 during the transport through the barriers.

The nuclides in Chain 4N+1 (Np-237 → U-233 → Th-229) will be solubility limited at the inlet of the finely ground rock, which will lead to lower release rates (Figure 6-10, Figure 6-3 and Table 6-2). Also the nuclides in Chain 4N+2 (Pu-242 → U-238 → U-234 → Th-230 → Ra-226), except Ra-226, will be solubility limited at the inlet of the finely ground rock. The difference in maximum release rate of Pu-242 with and without considering solubility limitations is small (Figure 6-11, Figure 6-4 and Table 6-2). This is explained by the fact that the maximum release rate in both cases is determined by the decay of Pu-242. The remaining nuclides in this decay chain will have lower release rates when solubility limitations are considered. The lower release rate of Ra-226 is due to the limitation in concentration of the parent nuclides.

Solubility limitations will also reduce the release rate of the nuclides in Chain 4N+3 (Pu-239 → U-235 → Pa-231) (Figure 6-12, Figure 6-5 and Table 6-2). Pa-231 will not be solubility limited in itself. It is the limitation in concentration of the parent nuclides that result in a lower release rate of Pa-231.

The difference between Figure 6-13 and Figure 6-6 shows the importance of the solubility limitations on the release of actinides and daughters. Most of the nuclides in the decay chains will be released from the bentonite-sand barrier at a significantly lower rate. The nuclides that will dominate the release of actinides and daughters when solubility limitations are considered are Np-237, U-233 and Pu-242.

Figure 6-14 shows the release rate from the bentonite-sand barrier of the dominating nuclides when solubility limitations are taken into account. During the first 10 000 years after canister breakthrough, C-14 will dominate the release. The maximum total release rate of activity is also obtained during this period. By comparing with Figure 6-7 it could be seen that the effect of solubility limitations is a lower level of total activity release, at times longer than a couple of thousand years.

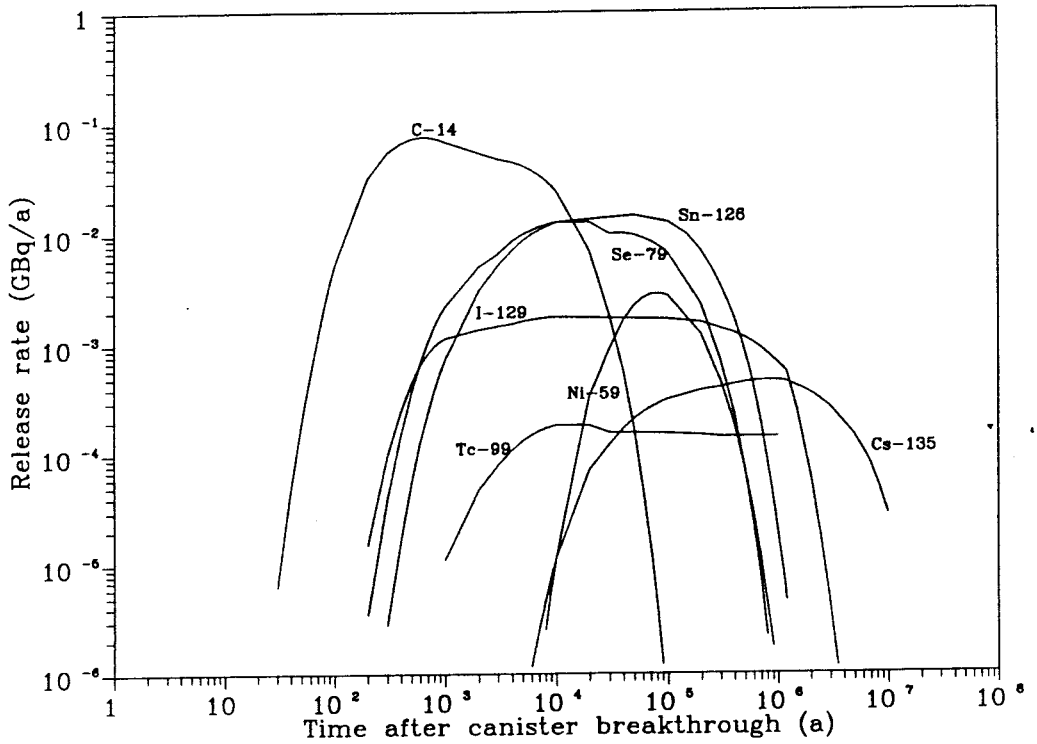

Figure 6-8: Release rates of fission and activation products from the bentonite-sand barrier versus time after canister breakthrough. Solubility limitations are considered.

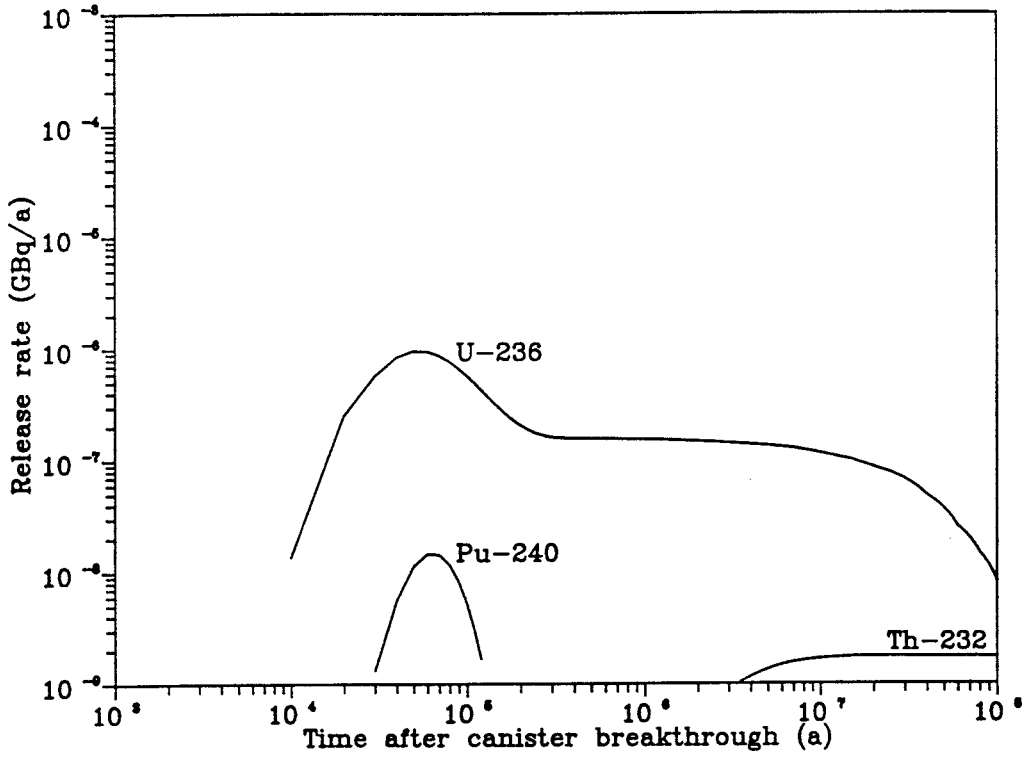

Figure 6-9: Release rates from the bentonite-sand barrier of nuclides in Chain 4N versus time after canister breakthrough. Solubility limitations are considered.

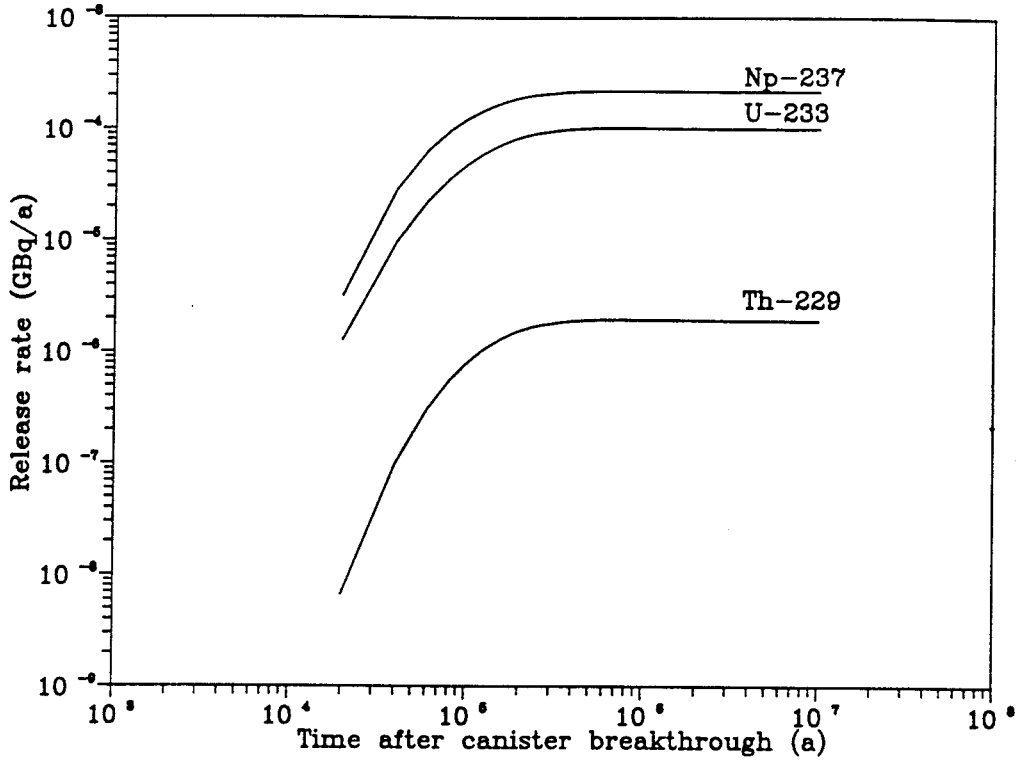

Figure 6-10: Release rates from the bentonite-sand barrier of nuclides in Chain 4N+1 versus time after canister breakthrough. Solubility limitations are considered.

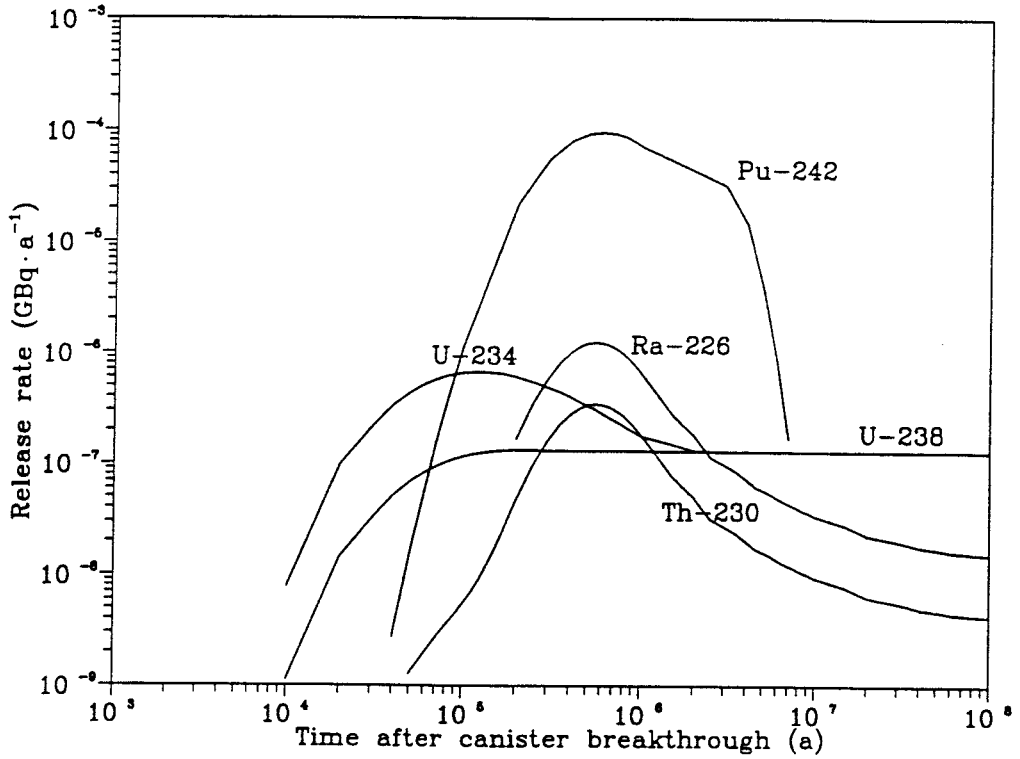

Figure 6-11: Release rates from the bentonite-sand barrier of nuclides in Chain 4N+2 versus time after canister breakthrough. Solubility limitations are considered.

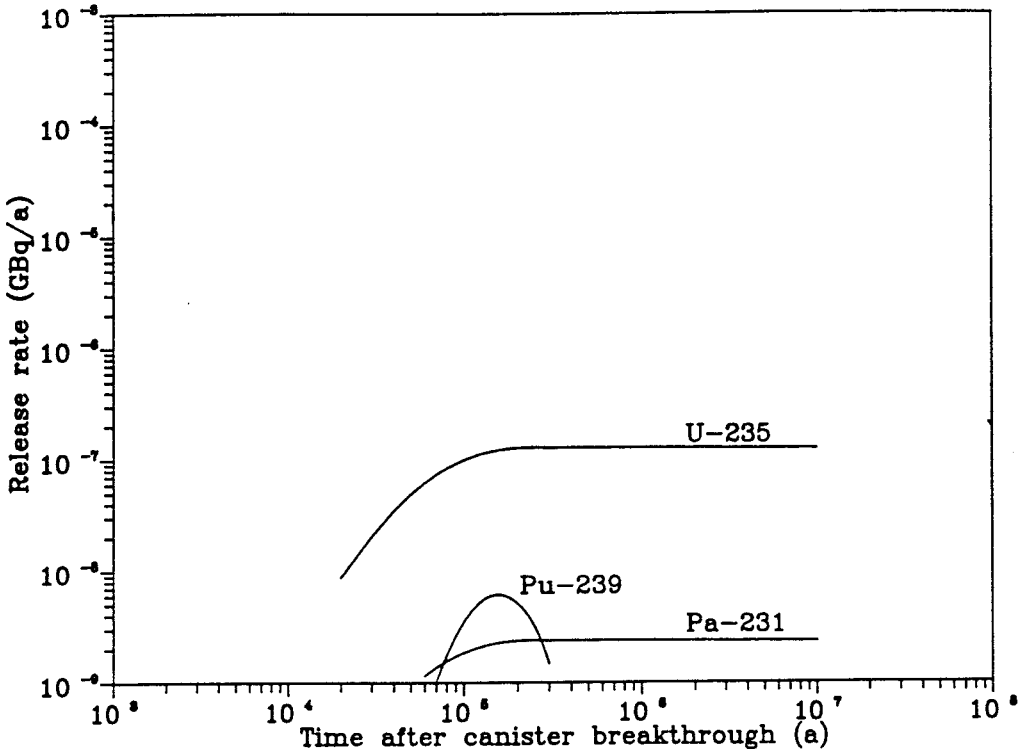

Figure 6-12: Release rates from the bentonite-sand barrier of nuclides in Chain 4N+3 versus time after canister breakthrough. Solubility limitations are considered.

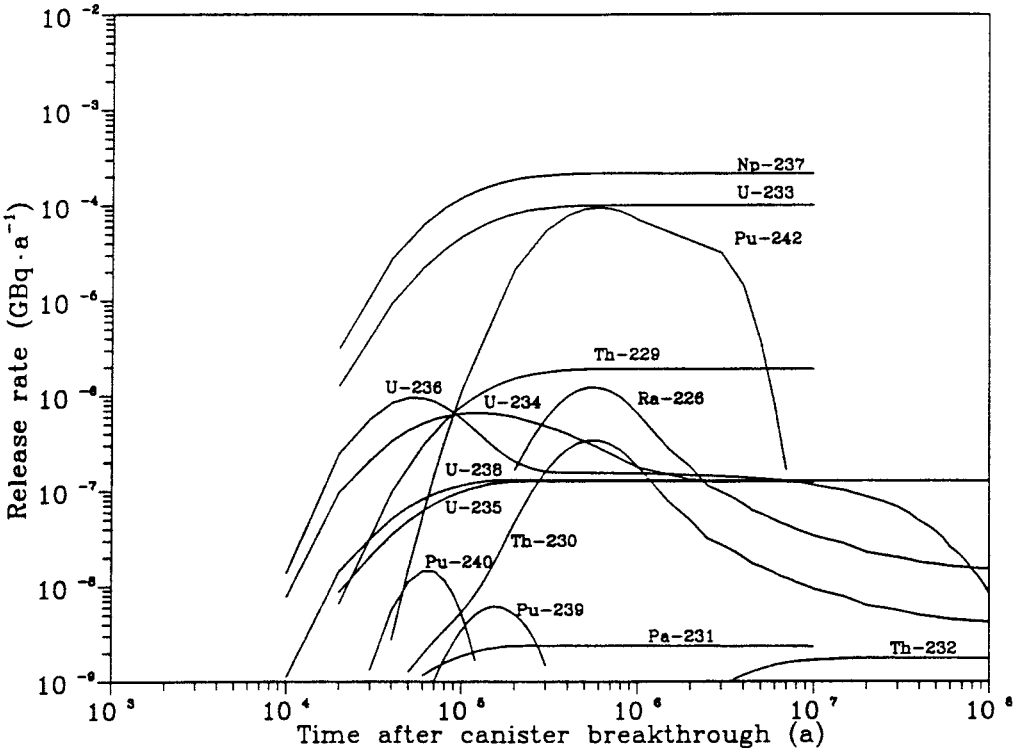

Figure 6-13: Release rates of actinides and daughters from the bentonite-sand barrier versus time after canister breakthrough. Solubility limitations are considered.

Table 6-2: Maximum release rate, corresponding time and reduction in maximum release rate when solubility limitations are considered.

Nuclide	Maximum release rate, (GBq · a^{-1})	Time after canister break-through, (a)	Reduction in max. release rate due to sol. limitations
Zr-93*	$< 10^{-7}$	$1.0 \cdot 10^{7}$	> 60 000
Tc-99	$1.8 \cdot 10^{-4}$	10 000	1 300
Pd-107	$5.4 \cdot 10^{-7}$	10 000	7 800
Ra-226	$1.2 \cdot 10^{-6}$	550 000	69
Th-229	$1.9 \cdot 10^{-6}$	400 000	24
Th-230	$3.4 \cdot 10^{-7}$	550 000	68
Th-232	$1.7 \cdot 10^{-9}$	$1.0 \cdot 10^{7}$	18
Pa-231	$2.3 \cdot 10^{-9}$	160 000	360
U-233	$1.0 \cdot 10^{-4}$	450 000	23
U-234	$6.7 \cdot 10^{-7}$	120 000	1 900
U-235	$1.3 \cdot 10^{-7}$	250 000	340
U-236	$9.6 \cdot 10^{-7}$	50 000	700
U-238	$1.3 \cdot 10^{-7}$	200 000	4 400
Np-237	$2.2 \cdot 10^{-4}$	450 000	7
Pu-239	$6.1 \cdot 10^{-9}$	160 000	9 800
Pu-240	$1.5 \cdot 10^{-8}$	60 000	7
Pu-242	$9.6 \cdot 10^{-5}$	600 000	2

* A conservative estimate based on the maximum release rate obtained with a higher solubility concentration.

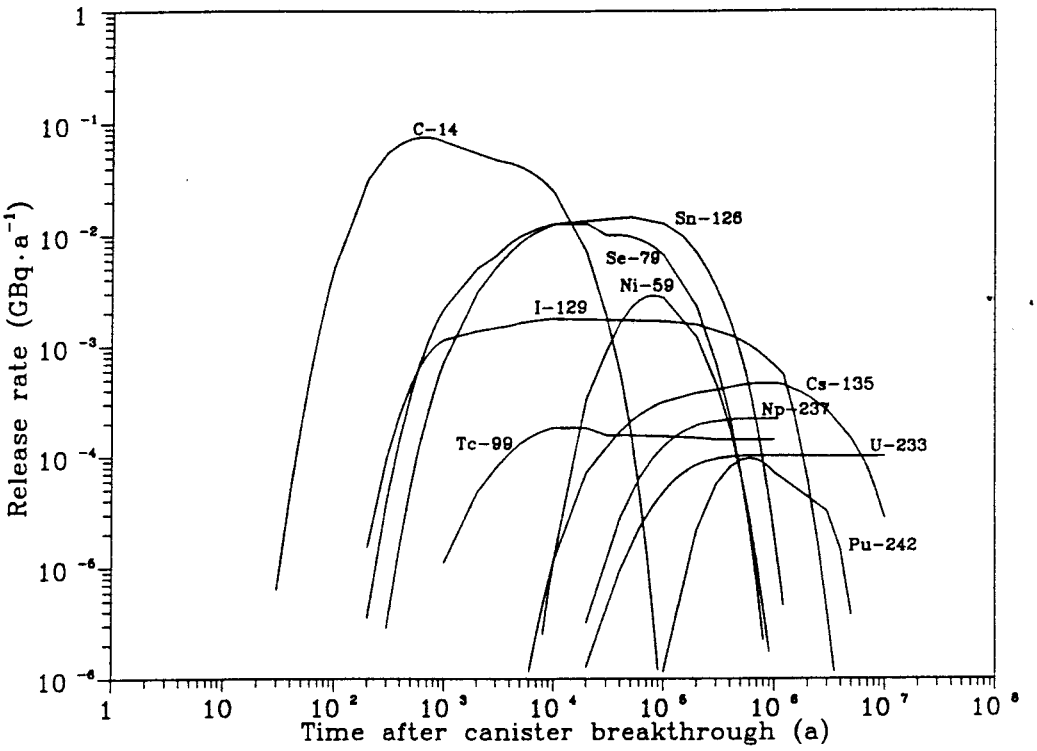

Figure 6-14: Release rates of dominating nuclides from the bentonite-sand barrier versus time after canister breakthrough. Solubility limitations are considered.

6.2 VARIATION CALCULATIONS, LOW FLOW THROUGH CASE

6.2.1 Effect of reducing the thickness of the bentonite-sand barrier

The effect of reducing the thickness of the bentonite-sand barrier on the steady state release of fission and activation products has been estimated. If the influence of the thermo-induced flow is neglected, equation (A.1) given in Appendix A can be used to estimate the increase in maximum release rate if the bentonite-sand barrier thickness is reduced from 5 to 2.5 metres. The result is presented in Table 6-3. The maximum release rate of the solubility limited Tc-99 and Pd-107 will be independent of the barrier thickness. The maximum release rate of I-129 will also be unaffected by the barrier thickness due to long half-life and low sorption ability in the barrier. The short lived and highly sorbing Nb-94 and the very short lived Sn-121m are the only nuclides among the fission and activation products that will be markedly affected by a reduction of the barrier thickness. Despite the large increase in maximum release rate, the contribution of Nb-94 and Sn-121m will not be of importance. The maximum release rate of the remaining fission and activation products from a 2.5 m thick barrier will be less than 5 times higher than the maximum release rate from a 5 m thick barrier.

The effect of the barrier thickness on the release of actinides and daughters has been determined by applying the calculation model described in Section 5.3. The results are shown in Figures 6-15 to 6-18 as the release rate from a 5 m thick (dashed line) and a 2.5 m thick (solid line) bentonite-sand barrier when solubility limitations are not considered. A significantly higher release rate from the 2.5 m thick barrier (more than one order of magnitude) is to be found only for the two rather short lived plutonium isotopes Pu-239 and Pu-240. The maximum release rate of the more long lived nuclides is less than 5 times higher from a 2.5 m thick barrier than from a 5 m thick barrier.

Table 6-3: Maximum release rates of fission and activation products from a 2.5 m thick bentonite-sand barrier and the ratio to the maximum release from a 5 metre thick barrier.

Nuclide	Release ratio $\frac{2.5\ \text{m}}{5\ \text{m}}$	Max. release rate, $(\text{GBq}\cdot\text{a}^{-1})$
C-14	1.5	$1.1\cdot10^{-1}$
Ni-59	3.2	$9.0\cdot10^{-3}$
Se-79	1.3	$1.7\cdot10^{-2}$
Zr-93	2.9	$1.7\cdot10^{-2}$
Nb-94	54	$1.0\cdot10^{-9}$
Tc-99	1.0	$1.8\cdot10^{-4}$
Pd-107	1.0	$5.4\cdot10^{-7}$
Sn-121m	16	$7.0\cdot10^{-9}$
Sn-126	1.1	$1.5\cdot10^{-2}$
I-129	1.0	$1.8\cdot10^{-3}$
Cs-135	1.2	$5.5\cdot10^{-4}$

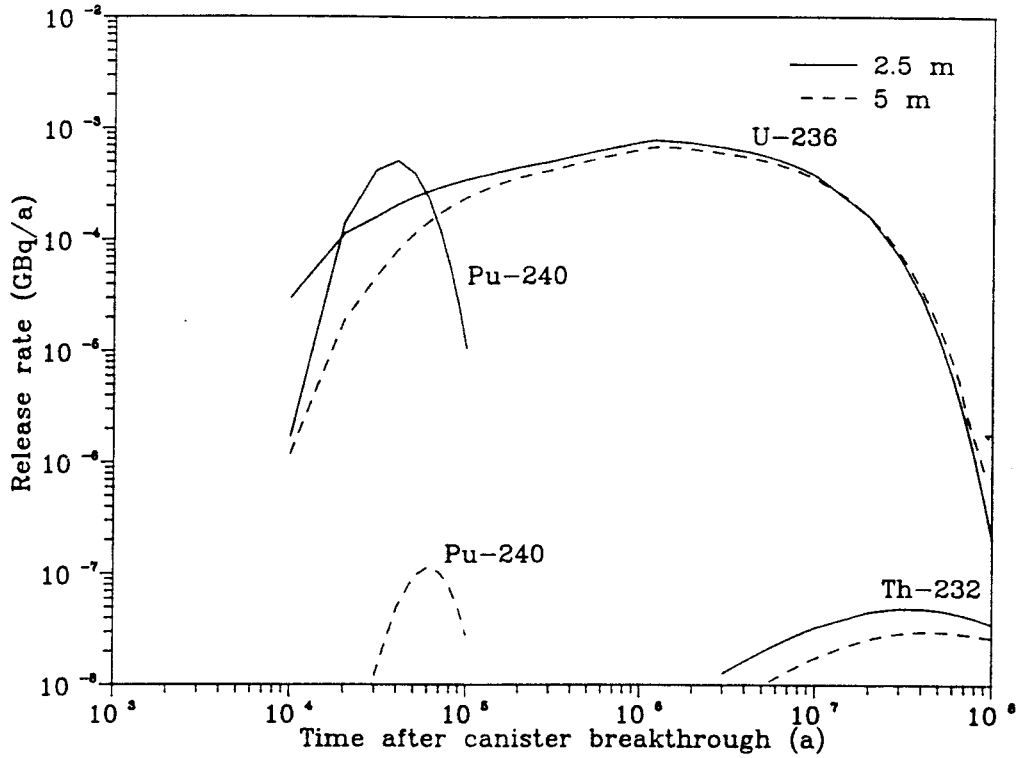

Figure 6-15: A comparison between the release rates from a 2.5 m and a 5 m thick bentonite-sand barrier. Nuclides in Chain 4N.

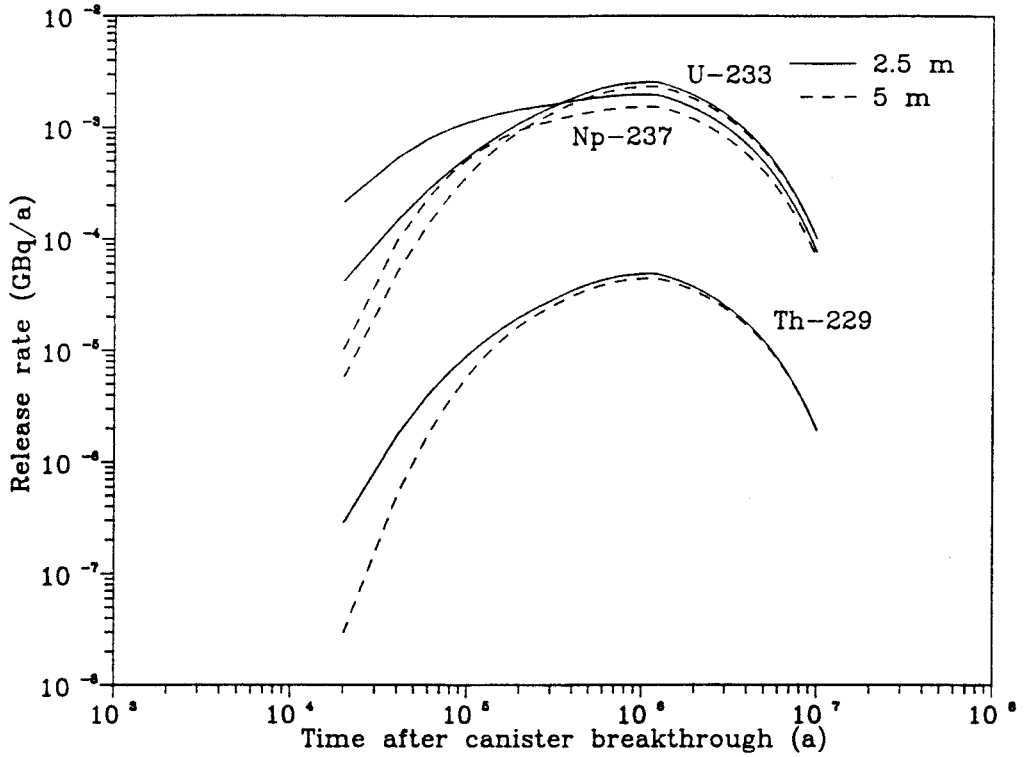

Figure 6-16: A comparison between the release rates from a 2.5 m and a 5 m thick bentonite-sand barrier. Nuclides in Chain 4N+1.

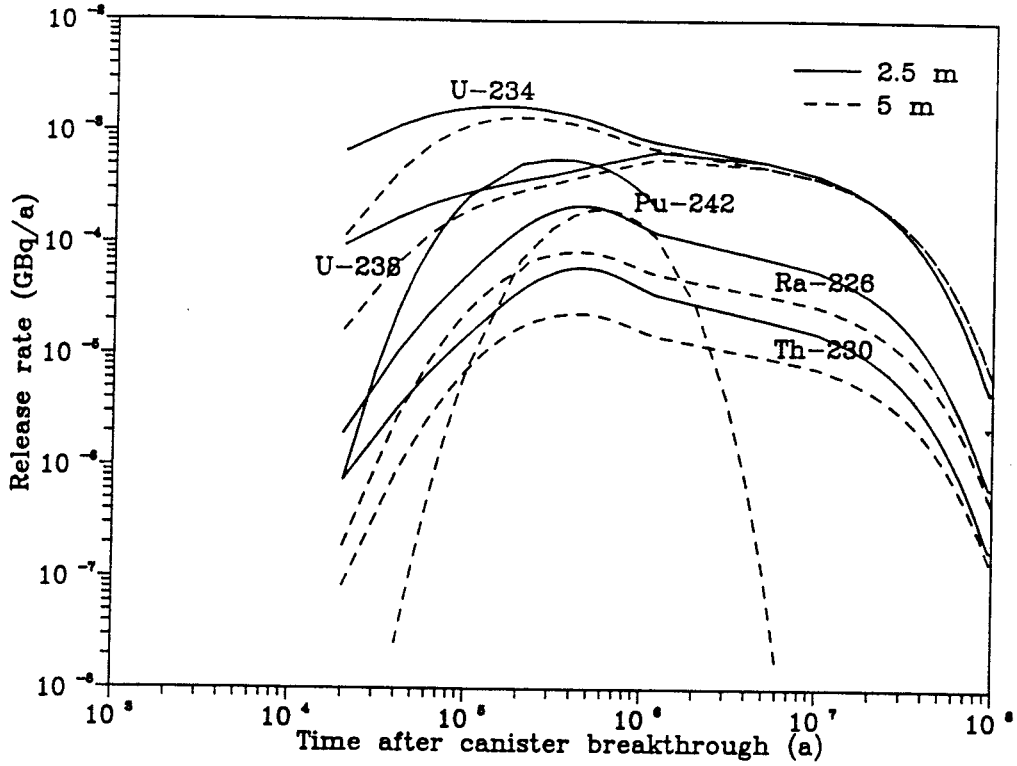

Figure 6-17: A comparison between the release rates from a 2.5 m and a 5 m thick bentonite-sand barrier. Nuclides in Chain 4N+2.

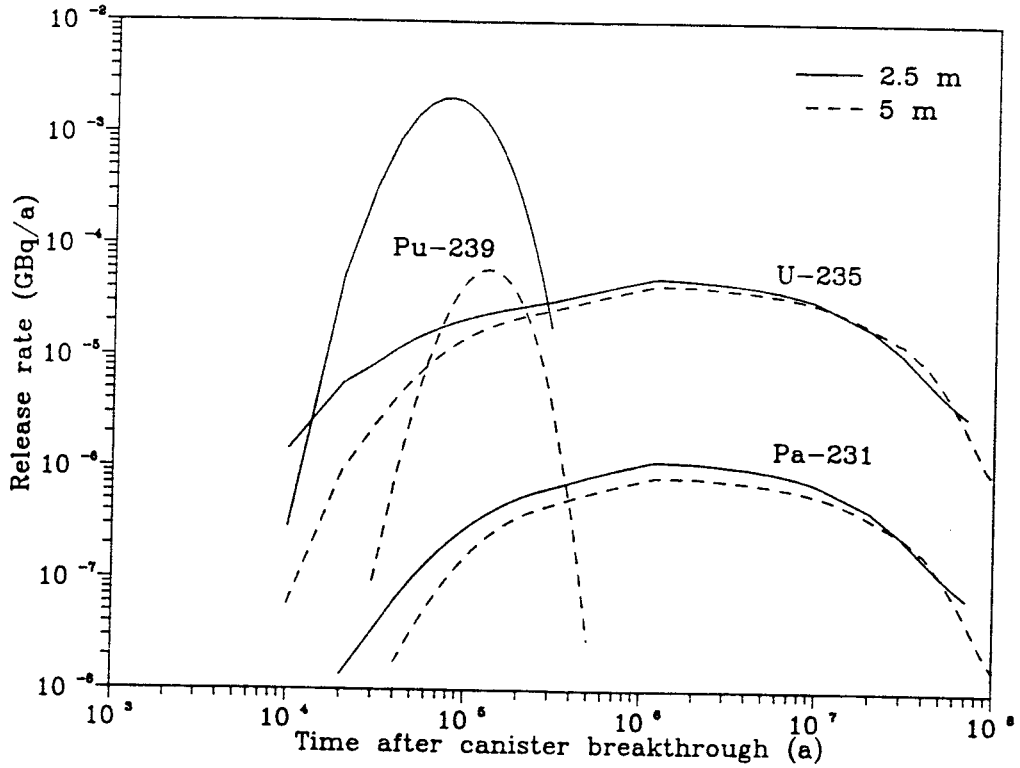

Figure 6-18: A comparison between the release rates from a 2.5 m and a 5 m thick bentonite-sand barrier. Nuclides in Chain 4N+3.

6.2.2 Effect of changing the sorption coefficient

The effect of the sorption on the release from the bentonite-sand barrier has been investigated for some of the nuclides for which the sorption data used in the previous presented calculations may be discussed. No solubility limitations have been included in these calculations.

The sorption coefficient for Sn and Pd in the bentonite-sand is in the central case assumed to be the same as for Tc, 0.0005 $m^3 \cdot kg^{-1}$. The release rate of Sn-126 and Pd-107, if sorption does not occur neither in the bentonite-sand nor in the finely ground rock, is shown in Figure 6-19 together with the curves obtained with the central case sorption values. The conservative assumption of no sorption at all in the barriers will result in higher maximum release rates, and the release will start earlier in time. The difference in maximum release rates is less than one order of magnitude.

The effect of lowering the uranium sorption in the finely ground rock has been calculated for the nuclides in Chain 4N+2 (Figure 6-20). A sorption coefficient of 1 $m^3 \cdot kg^{-1}$ compared to 5 $m^3 \cdot kg^{-1}$ will result in less than 5 times higher maximum release rate of U-238, U-234 and Th-230. The release of Ra-226, daughter of Th-230, is proportional to the release of Th-230. The increase in maximum release rate of Ra-226 will then also be less than a factor 5.

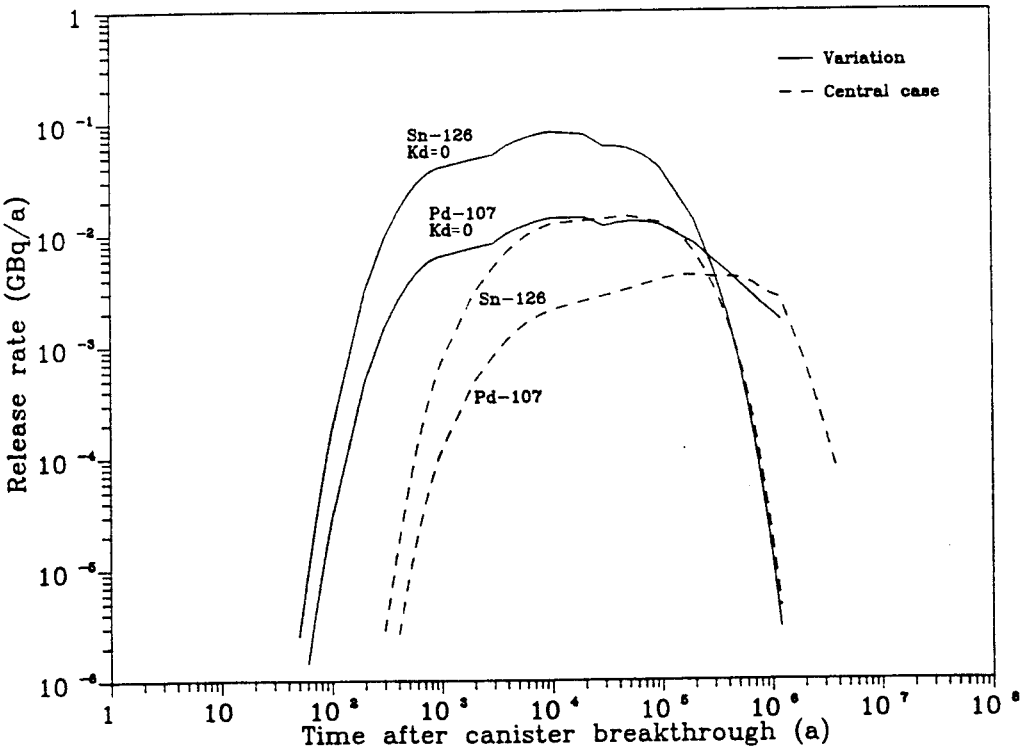

Figure 6-19: Release rates of Sn-126 and Pd-107 if no sorption in the barriers occurs (solid lines) in comparison with the release rates obtained with the sorption data assumed for the central case (dashed lines).

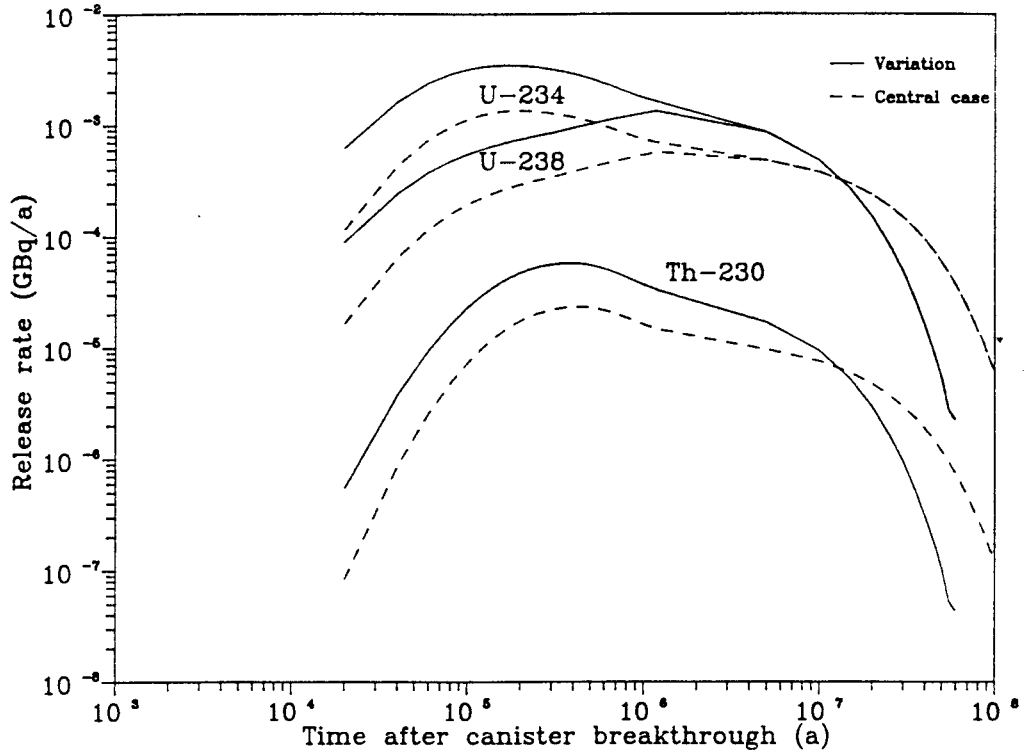

Figure 6-20: Release rates of nuclides in Chain 4N+2 obtained with a uranium sorption coefficient of 1 $m^3 \cdot kg^{-1}$ (solid lines) and 5 $m^3 \cdot kg^{-1}$ (dashed lines).

Data on sorption in the bentonite-sand used in the calculations presented so far are the same as were used in the safety analysis of the SFR repository. These data are valid for conditions where oxygen is present. In a WP-Cave repository the presence of ferrous iron ions, which are produced by the anaerobic corrosion of the iron canisters, will probably maintain reducing conditions also in the bentonite-sand barrier. Under reducing conditions, higher sorption of Tc, Pu, Np and U is expected in the bentonite-sand /Allard, 1988/ (Table 5-3).

The effect of a these higher sorption coefficients in the bentonite-sand barrier is exemplified in Figure 6-21 with the release rates of the nuclides in Chain 4N+1. The higher sorption coefficients for Np-237 and U-233 under reducing conditions will significantly delay the release of the nuclides in the chain. The maximum release rate of Np-237 and U-233 will decrease due to longer transport time through the barrier. Another effect of the longer transport time is that more Th-229 is produced in the barrier from decay of the parent nuclides. This will result in an increase of the maximum release rate of Th-229.

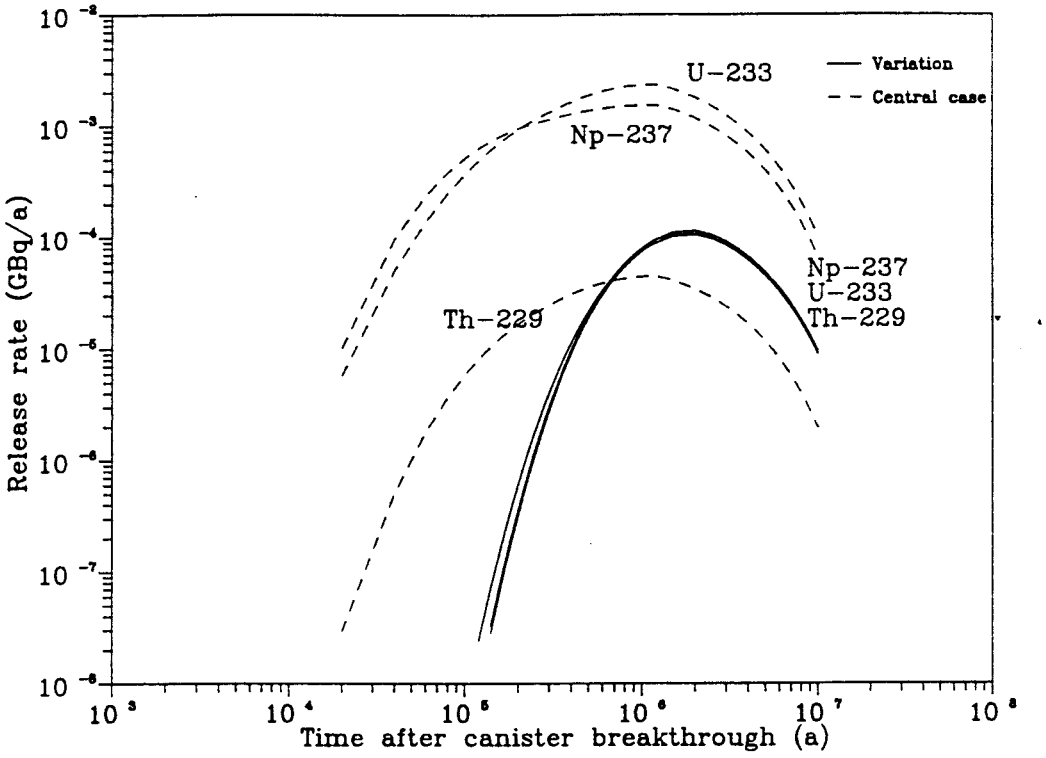

Figure 6-21: Release rates of nuclides in Chain 4N+1 when the uranium and neptunium sorption in the bentonite-sand is 0.3 $m^3 \cdot kg^{-1}$ (solid lines) in comparison with the release rates obtained with sorption data assumed for the central case (dashed lines).

6.2.3 Effect of increasing the radiolytic fuel oxidation rate

Nuclides which are solubility limited outside the canister surface with the fuel oxidation rate assumed in the main calculations will also be solubility limited with a higher fuel oxidation rate. Consequently, the maximum release rate of the solubility limited nuclides is not affected by an increase in fuel oxidation rate.

The dependence on the fuel oxidation rate for non-solubility limited radionuclides is exemplified in Figure 6-22. The Figure shows the release rate of carbon-14 with the fuel oxidation rate assumed in the main calculations (solid line), and the release rate with a 5 times higher oxidation rate, but without assuming that 10 % is immediately dissolved (broken line). In the latter case all fuel in the repository is oxidised after 20 000 years. The 5 times higher fuel oxidation rate results in a maximum release rate that is less than 2 times higher, approximately 0.12 GBq per year compared to 0.074 GBq per year. Assuming immediate dissolution of 10 % of the inventory will result in an earlier breakthrough, but the maximum release rate is not expected to be influenced. The effect on the maximum release rate of remaining important non-solubility limited nuclides is judged to be smaller than a factor of 2 since these nuclides have longer half-lives and/or a higher tendency to sorb in the barriers compared to carbon-14.

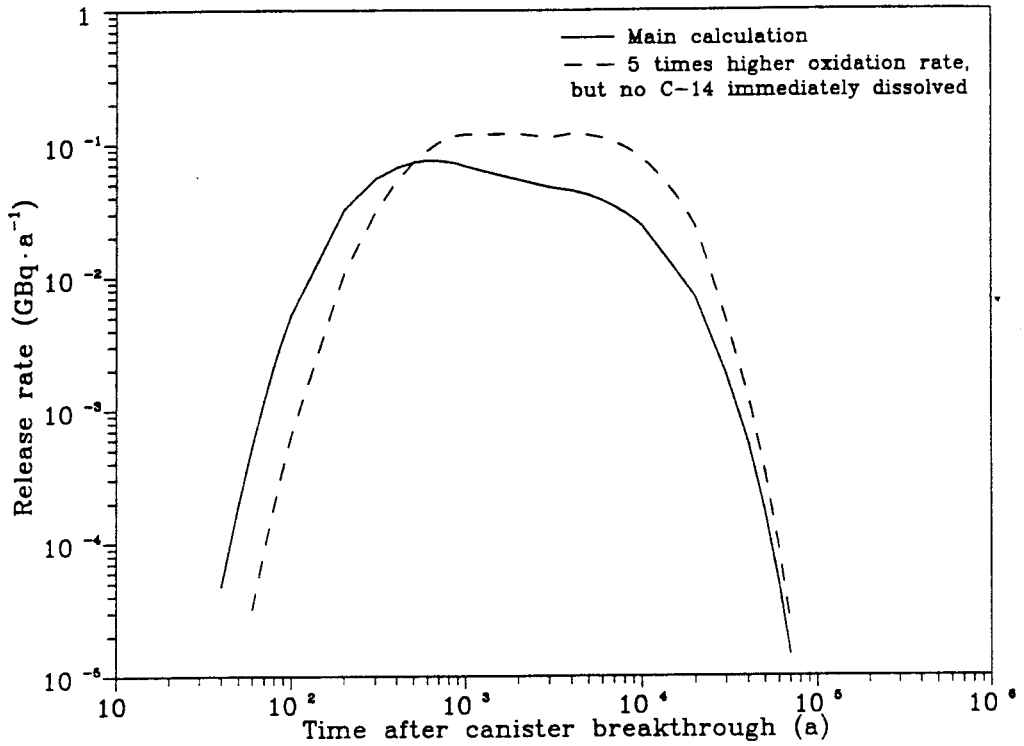

Figure 6-22: Effect of radiolytic fuel oxidation rate on the release rate of carbon-14. Solid line; fuel oxidation rate according to Figure 5-3. Broken line; 5 times higher than in Figure 5-3.

6.2.4 Effect of water flow rate in the rock outside the bentonite-sand barrier

The importance of the natural gradient driven water flow rate in the rock just outside the bentonite-sand barrier on the nuclide release from the barrier has been studied. A 10 times higher value, i.e., $3 \cdot 10^{-3}$ instead of $3 \cdot 10^{-4}$ $m^3 \cdot m^{-2} \cdot a^{-1}$, will increase the diffusive release rates approximately 3 times. The reason for this is that the resistance to diffusion from the outside of the barrier to the slowly moving water in the rock is inversely proportional to the square root of the velocity of the water passing the outside of the barrier. At times longer than about 5 000 years after canister breakthrough the release rate from the barrier is determined by this diffusion resistance. In this case, a 10 times higher water flow rate will result in about 3 times higher release rates from the barrier. At times up to 5 000 years after canister breakthrough the dominating release occurs by the thermally induced flow. During this time period, the increase in the release rates caused by a 10 times higher natural gradient driven water flow rate in the rock outside the barrier, is expected to be less than a factor of 3.

The importance of the direction of the water flow in the rock outside the barrier on the nuclide release occurring by diffusion has also been determined. The release rate of carbon-14 assuming a horizontal direction of the water flow was found to be about 15 % higher than in the case of a vertical direction of the flow.

6.3 HIGH FLOW THROUGH CASE

Calculations for the High Flow Through Case were performed for some selected radionuclides. The nuclides studied were C-14, Se-79, Sn-126, Ni-59, I-129, Cs-135, Pu-239, Pu-240, Pu-242 and Np-237. The release rate of Am-241 was also determined. This nuclide will decay to an insignificant level in the barriers in the Low Flow Through Case. This was found to be valid also for the High Flow Through Case since the maximum release rate was calculated to be less than 10^{-20} $GBq \cdot a^{-1}$.

Solubility limitations were considered in the calculations, and the nuclides that were found to have a release limited by their solubility were the plutonium isotopes and Np-237. After about 100 000 years the radiolytic fuel oxidation rate and the amount of plutonium left in the fuel were too low to give plutonium concentrations equal to the solubility limit. This was taken into account by letting the fuel oxidation rate determine the source term for the plutonium isotopes at times longer than about 100 000 years. For the remaining nuclides studied the same source term as in the Low Flow Through Case was used.

The release rate from the bentonite-sand barrier versus time after canister breakthrough for the studied nuclides is shown in Figure 6-23. The maximum release rate of each nuclide and the time when the maximum rate is obtained are given in Table 6-3 together with a comparison with the Low Flow Through Case. The higher water flow rate through the top of the bentonite-sand barrier in the High Flow Through Case will result in higher release rates compared to the Low Flow Through Case. Nuclides with relatively short half-life and/or low sorption in the barriers are most sensitive to the water flow rate through the bentonite-sand barrier. The immediate dissolution of 10 % of the inventory of carbon-14 and iodine-129 also contributes to the large difference in maximum release rate of these nuclides between the two cases.

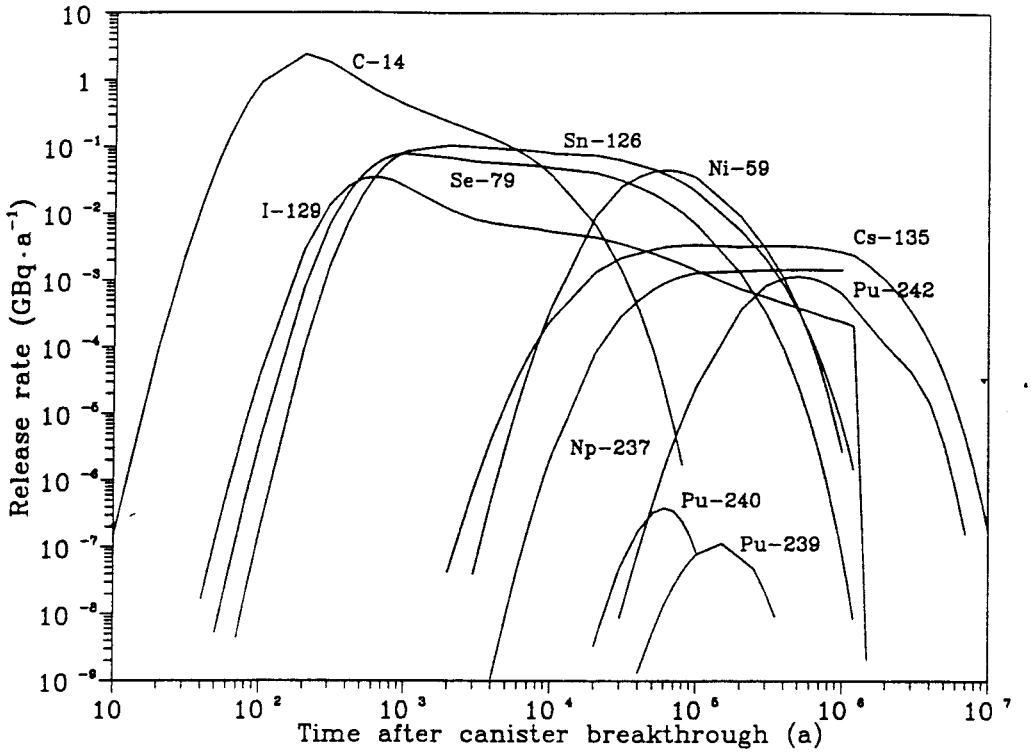

Figure 6-23: Release rates from the bentonite-sand barrier versus time after canister breakthrough in the High Flow Through Case. Solubility limitations are considered.

Table 6-3: Maximum release rate and corresponding time in the High Flow Through Case, and maximum release rate ratio High Flow Through to Low Flow Through Case. Solubility limitations are considered.

Nuclide	Maximum release rate, (GBq·a^{-1})	Time after canister break-through (a)	Maximum release rate ratio, High Flow to Low Flow Case
C-14	$2.4 \cdot 10^{0}$	200	32
Ni-59	$4.5 \cdot 10^{-2}$	60 000	16
Se-79	$7.7 \cdot 10^{-2}$	1 000	6
Sn-126	$1.0 \cdot 10^{-1}$	2 000	7
I-129	$3.4 \cdot 10^{-2}$	600	19
Cs-135	$3.4 \cdot 10^{-3}$	100 000	7
Pu-239	$1.1 \cdot 10^{-7}$	150 000	19
Pu-240	$3.9 \cdot 10^{-7}$	60 000	26
Pu-242	$1.1 \cdot 10^{-3}$	500 000	11
Np-237	$1.4 \cdot 10^{-3}$	400 000	6

7. DISCUSSION

The sorption data, nuclide diffusivities and solubilities used in the calculations presented in this report are valid for temperatures around 20 °C. The temperature in the refilled finely ground rock in the canister channels will after storage closure, however, reach a maximum of about 150 °C and then decrease to about 50 °C after a couple of thousand of years. Also the temperature in the bentonite-sand barrier will during a long period be well above 20 °C. Very limited information about sorption and solubilities at such high temperatures are at present available. This is the explanation to the selection of data for the calculations.

The solubilities used in the calculations will result in a limited release of many of the nuclides from the bentonite-sand barrier. All the solubility limited nuclides except Tc-99 and the plutonium isotopes have such long half-lives that they will reach steady state conditions. The release rate at steady state is directly proportional to the solubility. This means that if the solubilities at high temperatures are different from those used here, the release rate can be estimated by proportioning the release rate given here with the ratio of the solubilities. In the **Low Flow Through Case**, an upper limit is, however, given by the release rate obtained when no solubility limitations are considered.

An increase in radiolytic fuel oxidation rate will not affect the release of the solubility limited nuclides. Among the non-solubility limited nuclides that dominates the release from the bentonite-sand barrier, the short lived carbon-14 is the nuclide that will be most affected by the fuel oxidation rate. Increasing the fuel oxidation rate with a factor of 5 will result in an increase in maximum release rate of carbon-14 by a factor less than 2 in the **Low Flow Through Case.**

The sorption capacity in the barriers is also of importance for the release from the bentonite-sand barrier. In the previous section it was shown, for example, that the higher sorption coefficients of U and Np in the bentonite-sand under reducing conditions compared to oxidising conditions, result in a significantly lower release rate from the bentonite-sand barrier in the **Low Flow Through Case** if solubility limitations are not considered. In Figure 7-1 release curves for different combinations of sorption coefficients in the barriers are shown for the **Low Flow Through Case**. No radioactive decay is included, and the source term is 1 kg of an element that dissolves with the radiolytic fuel oxidation rate shown in Figure 5-3. Higher sorption coefficients results in later release and in lower maximum release rates. The lower maximum release rate is due to the decrease in element dissolution rate caused by the decrease in radiolytic fuel oxidation rate with time. This shows that sorption in the barriers is important for short lived nuclides but also for long lived nuclides that are not solubility limited.

Higher sorption coefficients will of course also result in later release of solubility limited nuclides. The effect of increasing the sorption coefficient in the bentonite-sand barrier from 0.006 to 0.3 $m^3 \cdot kg^{-1}$ is shown in Figure 7-2 by the two solid line curves. The sorption capacity in the finely ground rock is in both cases 5 $m^3 \cdot kg^{-1}$. The release curves are for a non-decaying species with a constant inlet concentration of $1 \cdot 10^{-3}$ $kg \cdot m^{-3}$. The later release obtained with the higher sorption capacity in the bentonite-sand barrier will be of importance for short lived nuclides.

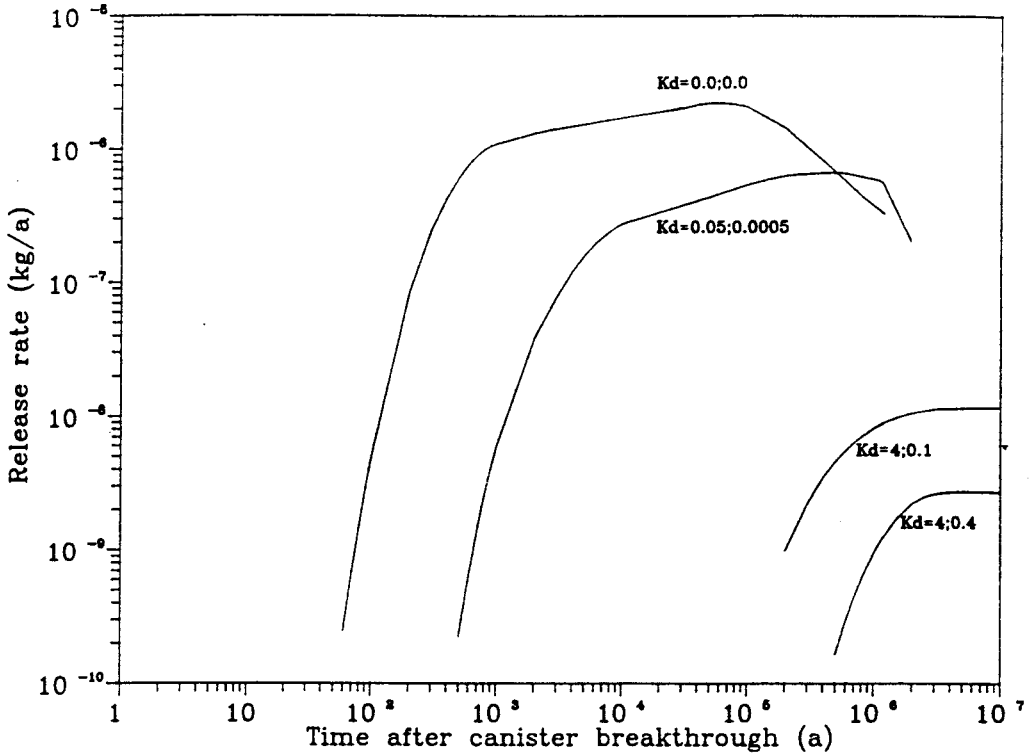

Figure 7-1: Release rate of a non-decaying species from the bentonite-sand barrier in the ***Low Flow Through Case*** *for different combinations of sorption coefficients in the finely ground rock (first value) and bentonite-sand barrier. Dissolution of 1 kg at a rate determined by the radiolytic fuel oxidation rate.*

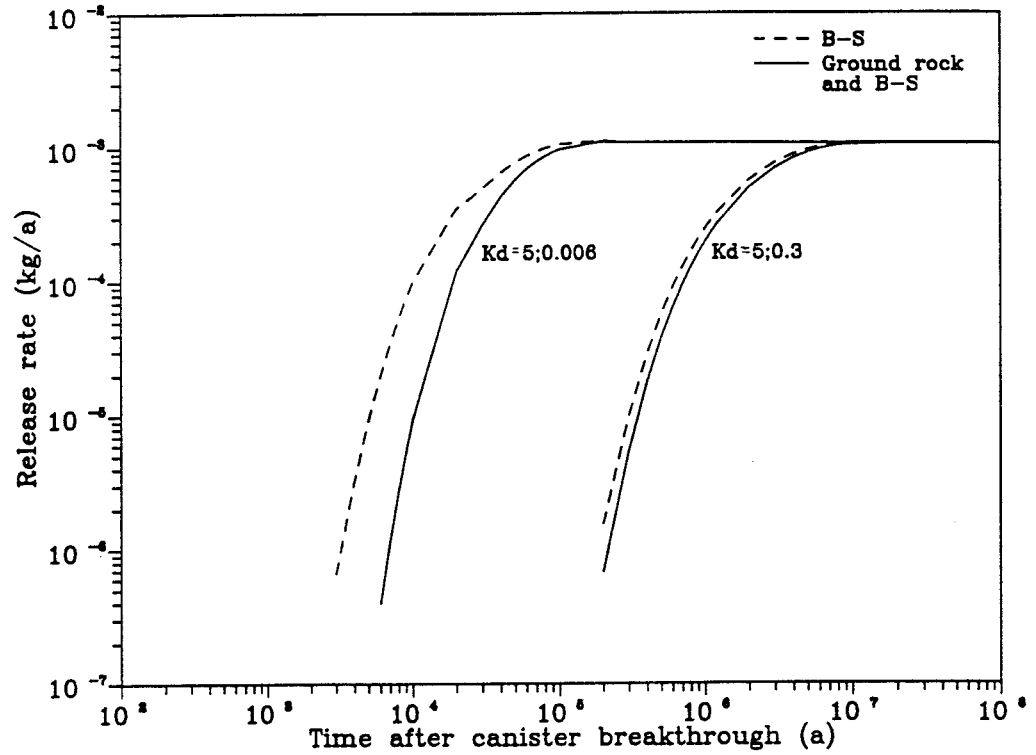

Figure 7-2: Release rates of a solubility limited non-decaying species in the ***Low Flow Through Case*** *for two combinations of sorption coefficients in the barriers. With and without the finely ground rock.*

The maximum release rate, which is obtained at steady state conditions, is independent of the sorption. The solubility limited nuclides that have long half-lives will reach steady state also with a higher sorption in the bentonite-sand, and the maximum release rate will be the same.

Figure 7-2 also shows the relative importance of the finely ground rock and the bentonite-sand barrier for a solubility limited species in the **Low Flow Through Case**. The effect of the sorption in the finely ground rock is small compared to the combined effect of sorption in the bentonite-sand and resistance to diffusion from the barrier to the flowing water outside the barrier. The combination of sorption capacities represents the maximum and minimum difference between the values in the finely ground rock and the bentonite-sand which have been used for a solubility limited nuclide in the release calculations.

For a non-solubility limited non-sorbing nuclide like carbon-14 the effect of the finely ground rock barrier on the release from the bentonite-sand barrier is negligible in the **Low Flow Through Case**. This is because the pore water capacity in the finely ground rock is not more than 0.5 % of the pore water capacity in the bentonite-sand barrier, and because the transport resistance due to diffusion in the finely ground rock is only 0.1 % of the transport resistance due to diffusion through the bentonite-sand barrier and diffusion from the barrier to the flowing water outside the barrier (Table 7-1). Only the bottom and cylindrical part of the bentonite-sand barrier is considered. The transport resistance in the barriers is defined as:

$$R = \frac{z}{D_p \varepsilon_p A} \qquad (7.1)$$

and the transport resistance outside the bentonite-sand barrier as:

$$R = \frac{1}{Q_{eq}} \qquad (7.2)$$

The reciprocal value of the transport resistance, the equivalent water flow, is a measure of the effectiveness of the barrier when steady state conditions are obtained. The values in Table 7-1 clearly show the importance of the resistance to diffusion from the bentonite-sand barrier to the flowing water outside the barrier in the **Low Flow Through Case**.

In the calculations presented in this report, the inner rock mass has not been included as a barrier. During the first 10^6 years after canister breakthrough the release from the bentonite-sand barrier will be dominated by the non-sorbing and slightly sorbing fission and activation products. The internal rock mass is not expected to significantly decrease the release of these nuclides since the capacity of the rock mass is small compared to the capacity in the other barriers. The amount of horizontal fissure openings in the inner rock mass is estimated to 0.42 metres on the whole height of the rock mass (250 metres) /Håkansson et al., 1988/, which

*Table 7-1: Pore water capacities and transport resistances in the finely ground rock and the bottom and cylindrical part of the bentonite-sand barrier in the **Low Flow Through Case**.*

Barrier	Pore water capacity (m^3)	Transport resistance ($s \cdot m^{-3}$)	Equivalent water flow, R^{-1} ($m^3 \cdot a^{-1}$)
Finely ground rock	540	36 800	860
Bentonite-sand	105 000	597 000	50
Diffusion-layer outside bentonite-sand		$3.5 \cdot 10^7$	0.91

would mean a flow porosity of $1.7 \cdot 10^{-3}$. With a total volume of the rock mass of $2 \cdot 10^6$ m^3 the initial capacity will be 3 400 m^3. Assuming a rock matrix porosity of $5 \cdot 10^{-3}$ will result in a final total capacity of 13 400 m^3 for a non-sorbing nuclide. With a flow porosity of 1%, the final capacity would be 30 000 m^3. Including the final capacity in the rock mass will, for a non-sorbing nuclide, result in an extra dilution volume in the order of 15 000-30 000 m^3 in addition to the dilution volume in the bentonite-sand barrier which is 105 000 m^3 (Table 7-1). Consequently, the release rates from the bentonite-sand barrier will be at most 10-25% lower than those obtained without considering the capacity in the rock mass. This shows the minor importance of the rock mass between the storage space and the bentonite-sand barrier on the release of non-sorbing nuclides.

At times longer than 10^6 years after canister breakthrough the solubility limited Np-237, Pu-242 and U-233 are among the nuclides that will dominate the release (Figure 6-14). The sorption in the rock mass between the storage space and the bentonite-sand barrier will probably decrease the maximum release rate of the rather short lived Pu-242. If the maximum release rate of the more long lived nuclides will be significantly affected by the retardation in the rock mass is difficult to predict without more information about the amount of fissure surfaces available to sorption and the flow situation in this part of the rock. The level of the maximum release rates of these nuclides is, however, one to two orders of magnitude lower than the level of maximum release rates of the non-sorbing and slightly sorbing fission and activation products that dominates during the first period. The far field transport when applying the channel theory will not reduce the maximum release rates of the non-sorbing fission and activation products /Moreno et al, 1989/, which means that the difference in maximum release rates from the far field in this case also will be one to two orders of magnitude or more. The importance of a further decrease in maximum release rate of the long lived solubility limited nuclides, which may be the result of the retardation in the rock mass, will then depend on whether the dose obtained from these nuclides is significant in comparison with the dose obtained from dominating non-sorbing fission and activation products.

The long lived nuclides that will dominate the release from the bentonite-sand barrier in a WP-Cave at long times are the same as those that will dominate the release from the near field in a KBS-3 repository /KBS-3, 1983/. The level of the maximum release rate of these nuclides in the **Low Flow Through Case** is also of the same magnitude when the release rate per canister is compared. The more short lived nuclides, which dominate the release from the bentonite-sand barrier in a WP-Cave repository during the first time period, will, in a KBS-3 repository, decay to an insignificant level before leaving the near field. This is the result of different canister materials. The long life time of the copper canisters in a KBS-3 repository will prevent the release of the short lived nuclides.

Comparing the results obtained in the 2 cases studied, the **Low Flow Through** Case and the **High Flow Through Case,** clearly shows that the hydraulic properties of the bentonite-sand barrier, and also to some extent the hydraulic properties of the inner rock mass, are very important to the release rate of nuclides from the bentonite-sand barrier. The hydraulic conductivity in the bentonite-sand barrier assumed in the High Flow Through Case, $1 \cdot 10^{-10}$ $m \cdot s^{-1}$, will result in a considerable water flow through the repository. Both the thermally induced water flow and the natural gradient driven water flow through the repository, and hence also the nuclide release rates from the bentonite-sand barrier, will be lower if a lower hydraulic conductivity in the bentonite-sand barrier could be achieved. A prolonged service life of the canisters would also diminish the effect of the thermally induced flow since this flow is decreasing with time.

8. CONCLUSIONS

The conclusions that can be drawn from this study can be summarised as follows:

- The release from the bentonite-sand barrier during the first 10^6 years after canister breakthrough will be dominated by some of the non-sorbing and slightly sorbing fission and activation products. The level of the maximum release rate during this period lies between 10^{-2} and 10^{-1} GBq·a^{-1} in the **Low Flow Through Case**, and around 2 to 3 GBq·a^{-1} in the **High Flow Through Case**. In both cases the maximum level is totally determined by the release rate of carbon-14.

- The release at longer times will be dominated by the long lived actinides and daughters. With the solubilities used here the level of the maximum release rate will not exceed 10^{-3} GBq·a^{-1} in the **Low Flow Through Case**, and will be about 10^{-3} GBq·a^{-1} in the **High Flow Through Case.**

- The hydraulic properties of the bentonite-sand barrier are very important to the release from the barrier. With the hydraulic conductivity assumed in the **Low Flow Through Case** the diffusion resistance outside the bentonite-sand barrier will play an important role by limiting the release of all nuclides from the bentonite-sand barrier. With a 10 times higher hydraulic conductivity in the bentonite-sand barrier, as in the **High Flow Through Case**, the nuclide release will be determined by the water flow through the barrier.

- The maximum release rate of the non-solubility limited nuclides and the short lived solubility limited nuclides will in the **Low Flow Through Case** be dependent on the sorption in the barriers, especially in the bentonite-sand barrier. Consequently, the maximum release rate of these nuclides will increase if the thickness of the bentonite-sand barrier is reduced. The increase in maximum release rate if the thickness of the bentonite-sand barrier is reduced from 5 to 2.5 metres will be less than a factor 5 for all important nuclides except Pu-239 and Pu-240 for which the increase will be markedly higher.

- The maximum release rate of solubility limited nuclides, with such long half-lives that steady state conditions are obtained, will not be dependent on the sorption in the barriers. Reducing the thickness of the bentonite-sand barrier will thus not influence the maximum release rate in the **Low Flow Through Case.**

- In the **High Flow Through Case** the water flow rate through a repository with a 2.5 m thick bentonite-sand barrier will be 2 times higher than through a repository with a 5 m thick barrier. Since the nuclide release from the barrier all the time is dominated by this water flow, the maximum release rates from a 2.5 m thick barrier will be about 2 times higher than from a 5 m thick barrier.

- A higher fuel oxidation rate will only influence the maximum release rate of the non-solubility limited nuclides. The nuclide that is expected to be most dependent on the fuel oxidation rate is the short lived, non-sorbing carbon-14, for which a 5 times higher fuel oxidation rate in the **Low Flow Through Case** results in an increase in maximum release rate by a factor less than 2.

- The rock mass between the storage space and the bentonite-sand barrier will not influence the maximum release rate from the bentonite-sand barrier of the non-sorbing and slightly sorbing nuclides that dominates during the first 10^6 years. The highly sorbing long lived nuclides that dominate at longer times may be affected if a large amount of fissure surfaces is available for sorption in that part of the rock. The importance of a possible lower maximum release rate of these long lived nuclides is dependent on the dose they give rise to in comparison with the dose obtained during the first time period from the non-sorbing and slightly sorbing nuclides.

LIST OF NOTATIONS

A	Cross sectional area in the transport direction (m^2)
A'	Area of the bottom and cylindrical part of the bentonite sand barrier (m^2)
A_T	Area of the top of the bentonite-sand barrier (m^2)
c_i	Liquid concentration of nuclide i ($kg \cdot m^{-3}$)
c_{i-1}	Liquid concentration of parent nuclide i-1 ($kg \cdot m^{-3}$)
$c_{i,sol}$	Solubility of nuclide i ($kg \cdot m^{-3}$)
$c_i(z_1)$	Concentration of nuclide i at the inlet boundary of the bentonite-sand barrier ($kg \cdot m^{-3}$)
$c_i(z_2)$	Concentration of nuclide i at the outlet boundary of the top of the bentonite-sand barrier ($kg \cdot m^{-3}$)
$c'_i(z_2)$	Concentration of nuclide i at the outlet boundary of the bottom and cylindrical part of the bentonite-sand barrier ($kg \cdot m^{-3}$)
D_a	Apparent diffusivity ($m^2 \cdot s^{-1}$)
D_p	Pore diffusivity ($m^2 \cdot s^{-1}$)
D_v	Diffusivity in bulk water ($m^2 \cdot s^{-1}$)
F	Radiolytic fuel oxidation rate ($kg \cdot s^{-1}$)
K_d	Sorption coefficient ($m^3 \cdot kg^{-1}$)
K_i	Sorption coefficient for nuclide i ($m^3 \cdot kg^{-1}$)
K_{i-1}	Sorption coefficient for parent nuclide i-1 ($m^3 \cdot kg^{-1}$)

L' Length of the water flow path outside the bottom and cylindrical part of the bentonite-sand barrier (m)

L_T Length of the water flow path outside the top part of the bentonite-sand barrier (m)

m_F Initial amount of fuel in the repository (kg)

m_i Amount of nuclide i in the fuel (kg)

m_i^0 Initial amount of nuclide i in the fuel (kg)

m_{i-1}^0 Initial amount of parent nuclide i-1 in the fuel (kg)

N_i Release rate of nuclide i from the fuel ($kg \cdot s^{-1}$)

N_i' Release rate of nuclide i from the bottom and cylindrical part of the bentonite-sand barrier ($kg \cdot s^{-1}$)

N_i^T Release rate of nuclide i from the top part of the bentonite-sand barrier ($kg \cdot s^{-1}$)

Q_{eq} Equivalent water flow ($m^3 \cdot s^{-1}$)

Q_{eq}' Equivalent water flow outside the bottom and cylindrical part of the bentonite-sand barrier ($m^3 \cdot s^{-1}$)

Q_{eq}^T Equivalent water flow outside the top part of the bentonite-sand barrier ($m^3 \cdot s^{-1}$)

R Retardation factor

R Transport resistance ($s \cdot m^{-3}$)

t Time (s)

u_0 Water flow rate in the rock outside the bentonite-sand barrier ($m^3 \cdot m^{-2} \cdot s^{-1}$)

v Water velocity in the top part of the bentonite-sand barrier ($m \cdot s^{-1}$)

z Length or length coordinate (m)

ε_f Flow porosity in the rock outside the bentonite-sand barrier ($m^3 \cdot m^{-3}$)

ε_p Porosity of the barriers ($m^3 \cdot m^{-3}$)

λ_i Decay constant for nuclide i (s^{-1})

λ_{i-1} Decay constant for parent nuclide i-1 (s^{-1})

ρ_s Solid density of the barriers ($kg.m^{-3}$)

REFERENCES

Allard B., Kipatsi H., Torstenfelt B., 1978,
"Sorption av Långlivade Radionuklider i Lera och Berg. Del 2", Chalmers University of Technology, KBS Technical Report 98, Stockholm, Sweden.

Allard B., Persson G., Torstenfelt B., 1985,
"Radionuclide Sorption on Carbonate-Clayish Rock", Radiochemistry Consultants group for Kemakta Consultants Co, NAGRA Technical Report 85-20, Baden, Switzerland.

Allard B., 1988,
Personal communication, University of Linköping, Sweden.

Andersson K., Torstenfelt B., Rydberg J., 1979,
"Leakage of Niobium-94 from an Underground Rock Repository", Chalmers University of Technology, KBS Technical Report 79-26, Stockholm, Sweden.

Baes C.F., Mesmer R.E., 1976,
"The Hydrolysis of Cations", John Wiley and Sons, New York, USA.

Christensen H., Bjergbakke E., 1987,
"SKB WP-Cave project - Radiolysis of Ground Water from Spent Fuel, stored according to the WP-Cave Concept", Studsvik Energiteknik AB, SKB AR 87-21, Stockholm, Sweden.

Edwards A. L., 1972,
"TRUMP: A Computer Program for Transient and Steady State Temperature Distribution in Multidimensional Systems", National Technical Information Service, National Bureau of Standards, Springfield Va, USA.

Grenthe I., 1989,
Personal communication, Department of Inorganic Chemistry, Royal Institute of Technology, Stockholm, Sweden.

Hopkirk R. J., 1988,
"SKB WP-Cave project - Thermally Induced Convective Motion in Groundwater in the Near Field of the WP-Cave after Filling and Closure", Polydynamics Limited, Zürich, Switzerland, SKB Technical Report 89-08, Stockholm, Sweden.

Håkansson U., Hässler L., Stille H., 1988,
"SKB WP-Cave projektet - WP-Cave, Bergmekaniska Aspekter - Analytiska beräkningar", Royal Institute of Technology, SKB AR 88-13, Stockholm, Sweden.

ITASCA, Consulting Group, Inc., May 1984,
"Three-dimensional groundwater flow patterns in the vicinity of a WP-Cave: Analysis and results", Minneapolis, USA.

Karlsson L-G., Höglund L-O., Pers K., 1986,
"Nuclide Release from the Near-Field of a L/ILW Repository", Kemakta Consultants Co., NAGRA Technical Report 85-33, Baden, Switzerland.

KBS-3, 1983,
"Final Storage of Spent Nuclear Fuel", Report by the Swedish Nuclear Fuel Supply Co., Stockholm, Sweden.

McKinley I. G., Hadermann J., 1985,
"Radionuclide Sorption Database for Swiss safety Assessment", Swiss Federal Institute for Reactor Research, NAGRA Technical Report '84-40, Baden, Switzerland.

Moreno L., Arve S., Neretnieks I., 1989,
"SKB WP-Cave project - Transport of escaping radionuclides from the WP-Cave repository to the biosphere", Royal Institute of Technology, SKB Technical Report 89-05, Stockholm, Sweden.

Neretnieks I., Andersson K., 1978,
"Utläckning av Ni-59 från ett Bergförvar", Royal Institute of Technology, KBS Technical Report 101, Stockholm, Sweden.

Neretnieks I., 1985,
"Diffusivities of some constituents in compacted wet bentonite clay and the impact on radionuclide migration in the buffer", Nucl. Techn., vol 71, p 458-470.

Werme L., 1988,
Personal communication, Swedish Nuclear Fuel and Waste Management Co SKB, Stockholm, Sweden.

Wiborgh M., Lindgren M., 1987,
"Database for the Radionuclide Transport Calculations for SFR", Kemakta Consultants Co, SKB Progress Report SFR 87-09, Stockholm, Sweden.

Appendix A

Identification of fission and activation products that decay to an insignificant level in the bentonite-sand barrier

The first selection of important fission and activation products was made based on the activity content of the nuclide in the fuel 300 years after discharge from reactor, and the toxicity of the nuclide. The result of this first selection is presented in Table A-1 as the identified nuclides, their half-lives and the activity content of each nuclide in the fuel (PWR-fuel, 38 000 $MWd \cdot tU^{-1}$) 300 years after discharge from reactor.

The second selection made was based on the effectiveness of the bentonite-sand barrier to retard the nuclides. Many of the nuclides presented in Table A-1 have rather short half-lives and will decay to an insignificant level before they are released from the bentonite-sand barrier. To sort out these nuclides, the maximum outflow from the bentonite-sand barrier of a nuclide relative to the inflow to the bentonite-sand barrier of the nuclide when the transport is diffusion, has been determined. If the outflow does not exceed 5 % of the inflow, the relative outflow is given by the equation /Neretnieks, 1985/:

$$\frac{N}{N_0} = e^{-\tau} \cdot \operatorname{erfc} \frac{H}{2\sqrt{\tau}} \tag{A.1}$$

$$\tau = \lambda \cdot t \tag{A.2}$$

$$H = z \cdot \sqrt{\lambda / D_a} \tag{A.3}$$

$$D_a = \frac{D_p \cdot \varepsilon_p}{\varepsilon_p + K_d \cdot \rho} \tag{A.4}$$

where

N = outflow of nuclide ($kg \cdot s^{-1}$)
N_0 = inflow of nuclide ($kg \cdot s^{-1}$)
t = time (s)
z = thickness of the barrier (m)
λ = decay constant (s^{-1})
D_a = apparent diffusivity ($m^2 \cdot s^{-1}$)
D_p = pore diffusivity ($m^2 \cdot s^{-1}$)
ε_p = porosity of the barrier
ρ = bulk density of the barrier ($kg \cdot m^{-3}$).
K_d = distribution coefficient ($kg \cdot kg^{-1} \cdot (kg \cdot m^{-3})^{-1}$).

Table A-1: Result of first selection of important fission and activation products.

Nuclide	Half-life(a)	Concentration in fuel, 300 years after discharge from reactor	
		GBq·metric ton^{-1}	grams·metric ton^{-1}
C-14	5730	25.9	0.16
Ni-59	75000	148	49.5
Ni-63	100	2590	1.23
Se-79	65000	17	6.61
Sr-90	28.8	2324	0.46
Y-90	*	2324	$1.2 \cdot 10^{-4}$
Zr-93	$1.5 \cdot 10^{6}$	74.7	803.6
Nb-93m	*	71	$6.8 \cdot 10^{-3}$
Nb-94	20000	0.006	$8.9 \cdot 10^{-4}$
Tc-99	214000	544.6	867.8
Pd-107	$6.5 \cdot 10^{6}$	5.3	280.2
Sn-121m	54.9	0.1	$6.4 \cdot 10^{-5}$
Sn-126	100000	33.7	32.1
Sb-126m	*	33.7	$1.2 \cdot 10^{-8}$
Sb-126	*	4.7	$1.5 \cdot 10^{-6}$
I-129	$16 \cdot 10^{6}$	1.4	206.6
Cs-135	$3 \cdot 10^{6}$	14.6	342.2
Cs-137	30.2	4274	1.3
Ba-137m	*	4044	$2.0 \cdot 10^{-7}$
Sm-151	90	1421	1.5
Ho-166m	1200	0.1	$1.9 \cdot 10^{-3}$

* Daughter in equilibrium with parent nuclide.

If the maximum relative outflow from the barrier (N_{max}/N_0) never exceeds 10^{-9}, the nuclide has decayed to an insignificant level in the barrier. By using equation (A.1), the maximum relative outflow obtained from a 5 meter thick bentonite-sand barrier was calculated. Since the effect of the barrier thickness on the radionuclide release is of interest, calculations for the case of a 2.5 meter thick barrier were also performed. The nuclides studied are those given in Table A-1. The calculations were made with sorption data, diffusivities, porosity and density of the barrier representative for a 10/90 bentonite-sand mixture (Table A-2). Most of the data are the same as those used in the SFR-study (Wiborgh and Lindgren, 1987).

Table A-2: Sorption and diffusivity data, 10/90 bentonite-sand. Reducing conditions. Bulk density = 2000 kg·m^{-3} (a), porosity = 0.25 (a).

Specie	K_d ($m^3 \cdot kg^{-1}$)	$D_e = D_p \cdot \varepsilon_p$ ($m^2 \cdot s^{-1}$)	D_a ($m^2 \cdot s^{-1}$)
C	0 (a)	$1.0 \cdot 10^{-10}$ (a)	$4.0 \cdot 10^{-10}$ (b)
Ni	0.025 (a)	$1.0 \cdot 10^{-10}$ (a)	$2.0 \cdot 10^{-12}$ (b)
Se	0.0003 (c)	$1.0 \cdot 10^{-10}$ (c)	$1.6 \cdot 10^{-11}$ (b)
Sr	0.032 (a)	$1.3 \cdot 10^{-9}$ (b)	$2.0 \cdot 10^{-11}$ (a)
Zr	0.40 (a)	$1.0 \cdot 10^{-10}$ (a)	$1.2 \cdot 10^{-13}$ (b)
Nb	0.1 (a)	$1.0 \cdot 10^{-10}$ (a)	$5.0 \cdot 10^{-13}$ (b)
Tc	0.0005 (a)	$1.0 \cdot 10^{-10}$ (a)	$9.8 \cdot 10^{-12}$ (b)
Pd	0 (d)	$1.0 \cdot 10^{-10}$ (e)	$4.0 \cdot 10^{-10}$ (b)
Sn	0 (d)	$1.0 \cdot 10^{-10}$ (e)	$4.0 \cdot 10^{-10}$ (b)
I	0.0003 (a)	$1.0 \cdot 10^{-10}$ (a)	$1.6 \cdot 10^{-11}$ (b)
Cs	0.025 (a)	$2.3 \cdot 10^{-10}$ (b)	$4.5 \cdot 10^{-12}$ (a)
Sm	0.25 (f)	$1.0 \cdot 10^{-10}$ (e)	$2.0 \cdot 10^{-13}$ (b)
Ho	0.25 (f)	$1.0 \cdot 10^{-10}$ (e)	$2.0 \cdot 10^{-13}$ (b)

(a) value from Wiborgh and Lindgren, 1987
(b) calculated by using equation A.3
(c) same as for I^- assumed according to McKinley and Hadermann, 1985
(d) same as in weathered rock assumed, McKinley and Hadermann, 1985
(e) assumed value
(f) same value as in both weathered rock and pure bentonite, from McKinley and Hadermann, 1985

The result of the calculation is presented in Table A-3 where the maximum relative outflow (N_{max}/N_0) of each nuclide is given as larger than 10^{-9} or less or equal to 10^{-9}. The nuclides that will decay to an insignificant level in the bentonite-sand barrier, 2.5 or 5 meter thick, are: Ni-63, Sr-90, Y-90 which is in equilibrium with Sr-90, Cs-137, Ba-137m daughter of Cs-137, Sm-151 and Ho-166m.

Table A-3: Maximum relative outflow of fission and activation products from a 10/90 bentonite-sand barrier.

Nuclide	2.5 m thick barrier		5 m thick barrier	
	$N_{max}/N_0>10^{-9}$	$N_{max}/N_0\leq10^{-9}$	$N_{max}/N_0>10^{-9}$	$N_{max}/N_0\leq10^{-9}$
C-14	X		X	
Ni-59	X		X	
Ni-63		X		X
Se-79	X		X	
Sr-90		X		X
Y-90		X*		X*
Zr-93	X		X	
Nb-93m	X*		X*	
Nb-94	X		X	
Tc-99	X		X	
Pd-107	X		X	
Sn-121m	X		X	
Sn-126	X		X	
Sb-126m	X*		X*	
Sb-126	X*		X*	
I-129	X		X	
Cs-135	X		X	
Cs-137		X		X
Ba-137m		X*		X*
Sm-151		X		X
Ho-166m		X		X

* Daughter in equilibrium with parent nuclide

Appendix B

Identification of nuclides in the decay chains that decay to an insignificant level in the finely ground rock or bentonite-sand barrier

B1.1 INTRODUCTION

Some of the short lived nuclides in the beginning of the four decay chains will decay to an insignificant level during the transport through the finely ground rock and the bentonite-sand barrier. The four decay chains are illustrated in Figures B1-B4. In order to identify these nuclides, some initial calculations on the transport through the finely ground rock and the bentonite-sand barrier have been performed.

B1.2 MODEL USED IN THE CALCULATIONS

The transport mechanism in the finely ground rock is diffusion. In the bentonite-sand barrier the transport occurs by diffusion, and in the top part also by the thermo-induced flow. In these initial calculations only the diffusional transport through the barriers has been considered.

The equation used is an analytical solution to the diffusion equation for the case of diffusion through a semi-infinite medium. The concentration at a distance z from the inlet boundary is given by /Neretnieks, 1985/:

$$c = c_0 \cdot \frac{1}{2}\left[e^{-H} \cdot \mathrm{erfc}\left(\frac{H}{2 \cdot \sqrt{\tau}} - \sqrt{\tau} \right) + e^{H} \cdot \mathrm{erfc}\left(\frac{H}{2 \cdot \sqrt{\tau}} + \sqrt{\tau} \right) \right] \qquad \text{(B.1)}$$

$$H = z \cdot \sqrt{\lambda / D_a} \qquad \text{(B.2)}$$

$$D_a = \frac{D_e}{\varepsilon_p + K_d \cdot \rho_b} \qquad \text{(B.3)}$$

$$\tau = \lambda \cdot t \qquad \text{(B.4)}$$

where

c_0 = the concentration at the inlet of the material, $(kg \cdot m^{-3})$
λ = decay constant of the nuclide, (s^{-1})
D_a = apparent diffusivity in the material, $(m^2 \cdot s^{-1})$
D_e = effective diffusivity in the material, $(m^2 \cdot s^{-1})$
ε_p = porosity of the material, $(m^3 \cdot m^{-3})$
K_d = sorption coefficient, $(m^3 \cdot kg^{-1})$
ρ_b = bulk density of the material, $(kg \cdot m^{-3})$
t = time, (s)

As $\tau \rightarrow \infty$, equation (B.1) increases against the asymtotic value given by:

$$c = c_0 \cdot e^{-H} \qquad \text{(B.5)}$$

Equation (B.5) was used to calculate the maximum concentration of each nuclide at a distance from the inlet boundary corresponding to the thickness of the finely ground rock and the bentonite-sand barrier respectively. If the maximum concentration of a nuclide at this distance is found to be less than or equal to $10^{-9} \cdot c_0$, the nuclide will decay to an insignificant level during the transport through the barrier. Equation (B.5) was also used to calculate the distance from the inlet boundary where the maximum concentration is equal to $10^{-9} \cdot c_0$.

The calculation started with the first nuclide in a decay chain for which the activity content in the fuel 300 years after discharge from reactor together with the contribution from decay of parent nuclides are more than $3.7 \cdot 10^{-3}$ GBq·(ton fuel)$^{-1}$. If the maximum concentration at a distance corresponding to the outlet of the finely ground rock barrier is less than or equal to $10^{-9} \cdot c_0$, the nuclide will decay to an insignificant level before entering the bentonite-sand barrier. If the contribution from decay of this nuclide in the finely ground rock barrier is negligible compared to the initial amount of the daughter nuclide, the same diffusion distance in the barrier is available for the daughter nuclide. If the contribution is not negligible, the finely ground rock inlet boundary for the daughter nuclide is moved to the plane in the barrier where the maximum concentration of the parent nuclide equals $10^{-9} \cdot c_0$.

For those nuclides that do not decay to an insignificant level in the finely ground rock the same method was used to calculate the maximum concentration at the outlet of the bentonite-sand barrier. The effect of the previous transport through the finely ground rock was in this case, however, not considered.

B1.3 RESULTS

Chain 4N (see Figure B1).

Cm-244:
Starting nuclide of decay chain. The maximum concentration at the outlet of the 0.2 m thick finely ground rock barrier is $8.2 \cdot 10^{-13} \cdot c_0$. Cm-244 will decay to an insignificant level in the finely ground rock.

Pu-240:
Daughter of Cm-244. The additional amount from decay of Cm-244 in the finely ground rock is negligible compared to the initial activity of Pu-240. The maximum concentration at the outlet of the finely ground rock is $0.23 \cdot c_0$. The maximum concentration at the outlet of the 5 m thick bentonite-sand barrier is $2.4 \cdot 10^{-6} \cdot c_0$. Pu-240 will not decay to an insignificant level in the finely ground rock or in the bentonite-sand barrier.

Pu-236:
Starting nuclide of decay chain. The maximum concentration at the outlet of the finely ground rock is less than $10^{-30} \cdot c_0$. Pu-236 will decay to an insignificant level in the finely ground rock barrier.

U-232:
Daughter of Pu-236. Additional amount from decay of Pu-236 in the finely ground rock is negligible compared to the initial amount of U-232. The maximum concentration at the outlet of the finely ground rock is $8.8 \cdot 10^{-7} \cdot c_0$. The maximum concentration at the outlet of the bentonite-sand barrier is $5.4 \cdot 10^{-14} \cdot c_0$. U-232 will decay to an insignificant level in the bentonite-sand barrier.

Conclusions Chain 4N:
The short lived nuclides Cm-244, Pu-236 and U-232 in the beginning of the decay chain will decay to an insignificant level during the transport through the barriers.

Chain 4N+1 (See Figure B2).

Cm-245:
Starting nuclide of decay chain. The maximum concentration at the outlet of the finely ground rock is $0.28 \cdot c_0$. The maximum concentration at the outlet of the bentonite-sand barrier is $3.4 \cdot 10^{-18} \cdot c_0$. To decrease the maximum concentration to $10^{-9} \cdot c_0$, a 2.6 m thick bentonite-sand barrier is required. Cm-246 will decay to an insignificant level in the bentonite-sand barrier.

Pu-241:
Daughter of Cm-245. The initial amount of Pu-241 will decay to an insignificant level in 0.1 m finely ground rock. Additional amount from decay of Cm-245 is, however, not negligible. The parent nuclide Cm-245 will decay to an insignificant level in the bentonite-sand barrier at a distance 2.6 m from the inlet. An additional 0.4 m is required to decrease the maximum concentration of Pu-241 to $10^{-9} \cdot c_0$. Pu-241 will decrease to an insignificant level in the bentonite-sand barrier at a distance (2.6+0.4)= 3 m from the inlet.

Am-241:
Daughter of Pu-241. The parent nuclide Pu-241 will decay to an insignificant level in the bentonite-sand barrier at a distance 3 m from the inlet. A 0.6 m thick bentonite-sand barrier is required to decrease the maximum concentration of Am-241 to $10^{-9} \cdot c_0$. Am-241 will then decay to an insignificant level in a (3+0.6) = 3.6 m thick bentonite-sand barrier.

Np-237:
Daughter of Am-241. The parent nuclides will decay to an insignificant level in the bentonite-sand barrier, 3.6 m from the inlet. The remaining 1.4 m of the bentonite-sand barrier will reduce the concentration of Np-237 to $0.93 \cdot c_0$. Np-237 will not decay to an insignificant level in the bentonite-sand barrier.

Conclusions Chain 4N+1:
The nuclides Cm-245, Pu-241 and Am-241 will decay to an insignificant level during the transport through the finely ground rock and the bentonite-sand barrier.

Chain 4N+2 (see Figure B3).

Cm-246:
Starting nuclide of decay chain. The maximum concentration at the outlet of the finely ground rock is $0.18 \cdot c_0$. To decrease the maximum concentration to $10^{-9} \cdot c_0$, 1.9 m bentonite-sand barrier is required. Cm-246 will decay to an insignificant level in the bentonite-sand barrier.

Am-242m:
Starting nuclide of decay chain. The maximum concentration at the outlet of the finely ground rock is $6.8 \cdot 10^{-5} \cdot c_0$. To decrease the maximum concentration to $10^{-9} \cdot c_0$, 0.3 m bentonite-sand barrier is required. Am-242m will decay to an insignificant level in the bentonite-sand barrier.

Am-242:
Daughter to Am-242m. Due to short half-life, in equilibrium with Am-242m. Am-242 will decay to an insignificant level in the bentonite-sand barrier.

Pu-242:
Daughter of Cm-246 and Am-242 (Am-242m). The additional amount from decay of parent nuclides in the barriers is negligible compared to the initial amount of Pu-242. The maximum concentration at the outlet of the finely ground rock is $0.82 \cdot c_0$. The maximum concentration at the outlet of the bentonite-sand barrier is $0.18 \cdot c_0$. Pu-242 will not decay to an insignificant level during the transport through the finely ground rock and the bentonite-sand barrier.

Cm-242:
Daughter of Am-242 (Am-242m). Additional amount from decay of parent nuclides is not negligible. The parent nuclides will decay to an insignificant level in the bentonite-sand barrier at a distance 0.3 m from the inlet. An additional 0.02 m bentonite-sand barrier is required to decrease the maximum concentration of Cm-242 to $10^{-9} \cdot c_0$. Cm-242 will decrease to an insignificant level in the bentonite-sand barrier.

Pu-238:
Daughter of Cm-242. The parent nuclide will decay to an insignificant level in the bentonite-sand barrier at a distance of 0.32 m from the inlet. To decrease the maximum concentration of Pu-238 to $10^{-9} \cdot c_0$, an additional 0.92 m bentonite-sand barrier is required. Pu-238 will decay to an insignificant level in the bentonite-sand barrier.

Conclusions Chain 4N+2:
The nuclides Cm-246, Am-242m, Am-242, Cm-242 and Pu-238 will decay to an insignificant level during the transport through the finely ground rock and the bentonite-sand barrier.

Chain 4N+3 (see Figure B4).

Am-243:
Starting nuclide of decay chain. Maximum concentration at the outlet of the finely ground rock barrier is $0.25 \cdot c_0$. Maximum concentration at the outlet of the bentonite-sand barrier is $1.8 \cdot 10^{-19} \cdot c_0$. To decrease the maximum concentration to $10^{-9} \cdot c_0$, 2.4 m bentonite-sand barrier is required. Am-243 will decay to an insignificant level in the bentonite-sand barrier.

Np-239:
Daughter to Am-243 and due to short half-life, in equilibrium with Am-243. Np-239 will decay to an insignificant level in the bentonite-sand barrier.

Cm-243:
Starting nuclide of decay chain. The maximum concentration at the outlet of the finely ground rock barrier is $2.9 \cdot 10^{-10} \cdot c_0$. Cm-243 will decay to an insignificant level in the finely ground rock.

Pu-239:
Daughter of Np-239 (Am-243) and Cm-243. The parent nuclides will decay to an insignificant level in the bentonite-sand barrier 2.4 m from the inlet. The remaining 2.6 m bentonite-sand barrier will reduce the maximum concentration of Pu-239 to $0.03 \cdot c_0$. Pu-239 will not decay to an insignificant level in the bentonite-sand barrier.

Conclusions Chain 4N+3:
The nuclides Am-243, Np-239 and Cm-243 will decay to an insignificant level during the transport through the finely ground rock and the bentonite-sand barrier.

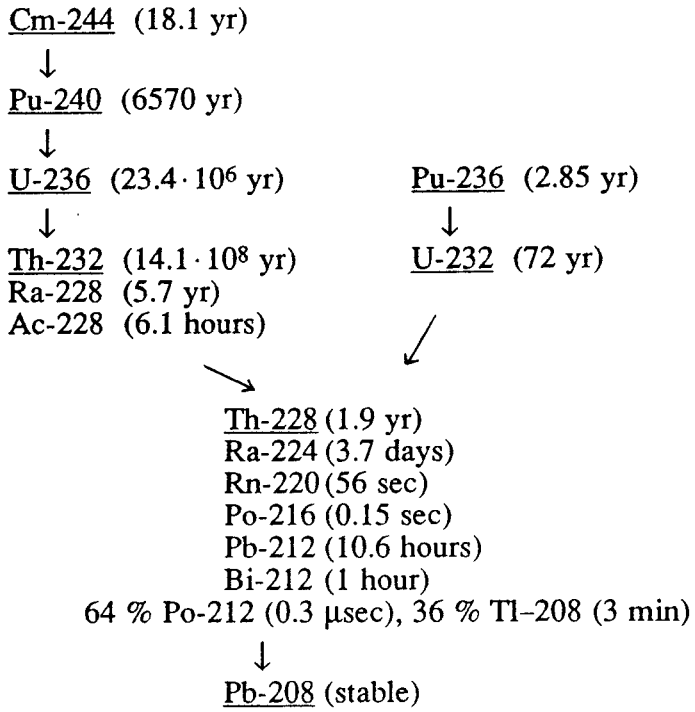

Figure B1: Chain 4N

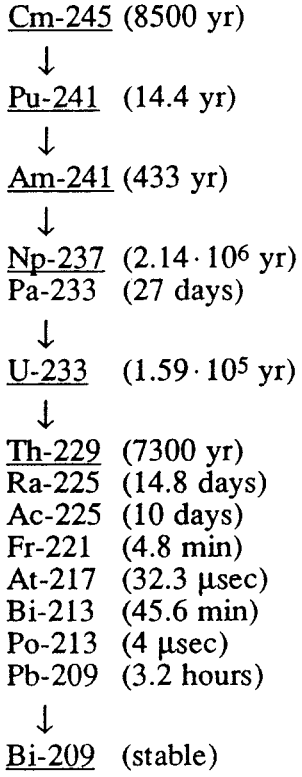

Figure B2: Chain 4N+1

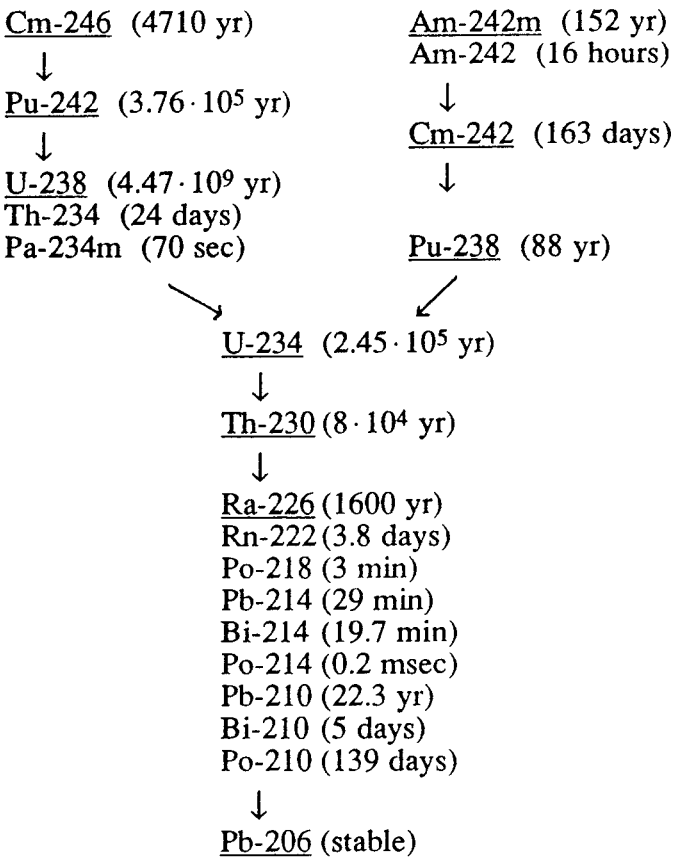

Figure B3: Chain 4N+2

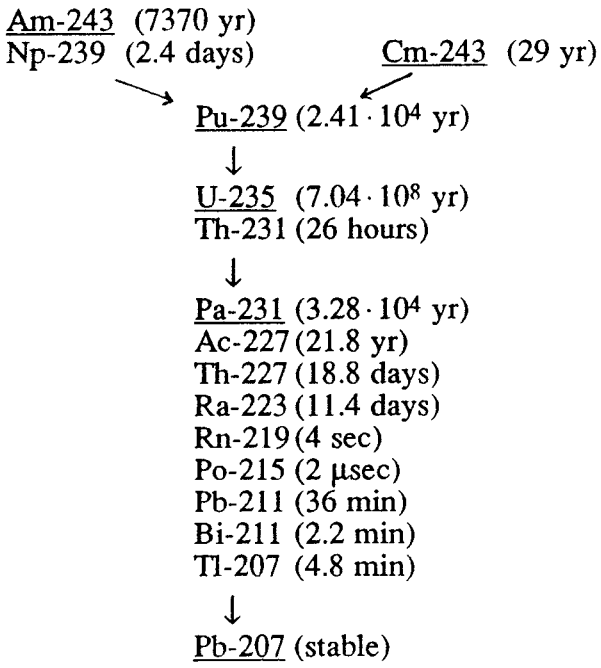

Figure B4: Chain 4N+3

Appendix C

Calculation of the groundwater flux driven by the natural gradient through the repository

In the calculation of the natural gradient driven water flow through the repository, the cave has been simulated by a system of two zones with constant but different hydraulic conductivities in an infinite medium, bounded by spherical surfaces. The innermost zone represents the internal rock mass and it is surronded by a zone representing the bentonite-sand barrier. The infinite medium represents the rock mass outside the bentonite-sand barrier where the water flux is q_0 $m^3 \cdot m^{-2} \cdot s^{-1}$.

The water flux, Q, through the innermost sphere is given by /ITASCA, 1984/:

$$Q = \frac{k_2 k_3 R_1^3}{(k_2+0.5k_3)(k_1+0.5k_2)R_1^3 - 0.5(k_2-k_3)(k_2-k_1)R_2^3} \cdot \frac{9}{4} \cdot \pi \cdot R_2^2 \cdot q_0 \qquad (C.1)$$

where

k_1 = permeability/hydraulic conductivity in the infinite medium
k_2 = permeability/hydraulic conductivity in bentonite-sand barrier
k_3 = permeability/hydraulic conductivity in the inner rock mass
R_1 = radius of the outermost sphere
R_2 = radius of the innermost sphere.

The following values of the parameters were used in the calculation of the natural gradient driven water flux through the repository in the **High Flow Through Case**:

$k_1 = 1 \cdot 10^{-9}$ $m \cdot s^{-1}$, $k_2 = 1 \cdot 10^{-10}$ $m \cdot s^{-1}$, $k_3 = 1 \cdot 10^{-7}$ $m \cdot s^{-1}$
$R_1 = 95$ m, $R_2 = 90$ m, $q_0 = 9.5 \cdot 10^{-12}$ $m^3 \cdot m^{-2} \cdot s^{-1}$.

The radii used are those of spheres that have the same projected area in the vertical plane as the WP-Cave repository, with and without the bentonite-sand barrier respectively.

With the above given data the water flux through the repository was calculated to $3.7 \cdot 10^{-7}$ $m^3 \cdot s^{-1}$ = 11.6 $m^3 \cdot a^{-1}$.

List of SKB reports

Annual Reports

1977–78
TR 121
KBS Technical Reports 1 – 120.
Summaries. Stockholm, May 1979.

1979
TR 79–28
The KBS Annual Report 1979.
KBS Technical Reports 79-01 – 79-27.
Summaries. Stockholm, March 1980.

1980
TR 80–26
The KBS Annual Report 1980.
KBS Technical Reports 80-01 – 80-25.
Summaries. Stockholm, March 1981.

1981
TR 81–17
The KBS Annual Report 1981.
KBS Technical Reports 81-01 – 81-16.
Summaries. Stockholm, April 1982.

1982
TR 82–28
The KBS Annual Report 1982.
KBS Technical Reports 82-01 – 82-27.
Summaries. Stockholm, July 1983.

1983
TR 83–77
The KBS Annual Report 1983.
KBS Technical Reports 83-01 – 83-76
Summaries. Stockholm, June 1984.

1984
TR 85–01
Annual Research and Development Report 1984
Including Summaries of Technical Reports Issued during 1984. (Technical Reports 84-01– 84-19)
Stockholm June 1985.

1985
TR 85-20
Annual Research and Development Report 1985
Including Summaries of Technical Reports Issued during 1985. (Technical Reports 85-01-85-19)
Stockholm May 1986.

1986
TR 86-31
SKB Annual Report 1986
Including Summaries of Technical Reports Issued during 1986
Stockholm, May 1987

1987
TR 87-33
SKB Annual Report 1987
Including Summaries of Technical Reports Issued during 1987
Stockholm, May 1988

1988
TR 88-32
SKB Annual Report 1988
Including Summaries of Technical Reports Issued during 1988
Stockholm, May 1989

Technical Reports

1989
TR 89-01
Near-distance seismological monitoring of the Lansjärv neotectonic fault region Part II: 1988
Rutger Wahlström, Sven-Olof Linder, Conny Holmqvist, Hans-Edy Mårtensson
Seismological Department, Uppsala University, Uppsala
January 1989

TR 89-02
Description of background data in SKB database GEOTAB
Ebbe Eriksson, Stefan Sehlstedt
SGAB, Luleå
February 1989

TR 89-03
Characterization of the morphology, basement rock and tectonics in Sweden
Kennert Röshoff
August 1988